JACS
JOURNAL OF THE AMERICAN CHEMICAL SOCIETY

Perspective

pubs.acs.org/JACS

New Methods and Applications in Solid-State NMR Spectroscopy of Quadrupolar Nuclei

Sharon E. Ashbrook* and Scott Sneddon

School of Chemistry, EaStCHEM, and Centre of Magnetic Resonance, University of St Andrews, St Andrews KY16 9ST, United Kingdom

ABSTRACT: Solid-state nuclear magnetic resonance (NMR) spectroscopy has long been established as offering unique atomic-scale and element-specific insight into the structure, disorder, and dynamics of materials. NMR spectra of quadrupolar nuclei ($I > {}^1/_2$) are often perceived as being challenging to acquire and to interpret because of the presence of anisotropic broadening arising from the interaction of the electric field gradient and the nuclear electric quadrupole moment, which broadens the spectral lines, often over several megahertz. Despite the vast amount of information contained in the spectral line shapes, the problems with sensitivity and resolution have, until very recently, limited the application of NMR spectroscopy of quadrupolar nuclei in the solid state. In this Perspective, we provide a brief overview of the quadrupolar interaction, describe some of the basic experimental approaches used for acquiring high-resolution NMR spectra, and discuss the information that these spectra can provide. We then describe some interesting recent examples to showcase some of the more exciting and challenging new applications of NMR spectra of quadrupolar nuclei in the fields of energy materials, microporous materials, Earth sciences, and biomaterials. Finally, we consider the possible directions that this highly informative technique may take in the future.

1. INTRODUCTION

Among the most important aims of the solid-state chemist is the ability to predict and control the properties of compounds and therefore to design a material (and the requisite synthetic route) specifically for a particular application. Key to this is an understanding of the structure-property-function relationships in the solid state, with the first, and perhaps most vital, step being a detailed structural characterization. Historically, this has been achieved using techniques based on Bragg diffraction, relying on the presence of the long-range order characteristic of many solids. While extremely powerful for ordered crystalline solids, diffraction typically produces a structural picture averaged over both time and length scales. As many of the interesting properties of solids (such as the activity of microporous catalysts, the radiation resistance and durability of ceramics, and the capacity of energy materials) arise from variation of this periodic nature, the use of spectroscopic techniques, which have the ability to probe the detailed atomic-scale structure, is a vital and yet often overlooked complementary approach. NMR spectroscopy has long been heralded as a sensitive probe of the local environment in solids. It can provide detailed information on structure and disorder in the solid state, while its sensitivity to motion over a wide range of time scales also enables dynamics to be investigated.[1,2] The use of ^{1}H, ^{13}C, ^{29}Si, and ^{31}P NMR spectroscopy has had a significant impact in the pharmaceutical industry, materials chemistry, geochemistry, and industrial chemistry for the study of drugs and active pharmaceuticals, catalysts, glasses, zeolites, and minerals.[3−10]

Unlike their solution-state counterparts, NMR spectra of solids are affected by anisotropic (or orientation-dependent) interactions, including chemical shift anisotropy (CSA) and dipolar coupling, preventing the extraction of site-specific information.[1,2] These interactions are averaged by molecular tumbling in solution, providing spectra with higher sensitivity and high resolution. Approaches for removing anisotropic broadening in the solid state, such as magic-angle spinning (MAS)[11] and decoupling,[12] are available, and for nuclei with spin quantum number $I = {}^1/_2$, high-resolution or isotropic spectra can be obtained. The NMR spectra of quadrupolar nuclei (i.e., those with $I > {}^1/_2$) are additionally affected by an interaction with the electric field gradient at the nucleus.[13,14] The anisotropic quadrupolar broadening can be significant, with line shapes broadened over many megahertz. Furthermore, this anisotropy cannot be removed completely by MAS, so the spectra remained broadened even when the sample is rotated.[13,14] Although in principle the quadrupolar interaction provides an additional probe of the local structure and geometry, more usually the anisotropic broadening prevents the resolution of distinct line shapes and makes the acquisition of detailed information significantly more challenging.

Over 74% of the nuclides in the periodic table have spin quantum number $I > {}^1/_2$, and for over 63% of the elements the only NMR-active isotopes are quadrupolar, meaning that there are no $I = {}^1/_2$ counterparts available for study. However, quadrupolar nuclei, such as ^{2}H, $^{6/7}$Li, ^{11}B, ^{14}N, ^{17}O, ^{23}Na, ^{25}Mg, ^{27}Al, ^{35}Cl, ^{39}K, ^{59}Co, $^{69/71}$Ga, and ^{93}Nb, are of importance across the fields of chemistry, physics, biology, materials science, and geology, as they are present in inorganic oxides, functional materials and ceramics, glasses and clays, polymers, pharmaceuticals and biomaterials, energy materials, and the compounds that make up the inner layers of our own planet.[1,2,14−20] The development of methods to study these nuclei using NMR spectroscopy and the ability to exploit the site-specific and atomic-scale structural information this provides is therefore crucial.

Received: May 12, 2014
Published: October 8, 2014

   dx.doi.org/10.1021/ja504734p | J. Am. Chem. Soc. 2014, 136, 15440−15456

In this Perspective, after briefly reviewing the quadrupolar interaction, the experimental approaches used to acquire NMR spectra of quadrupolar nuclei, and the methods used to achieve high resolution, we will consider how NMR spectroscopy of quadrupolar nuclei can provide information on structure, disorder, dynamics, and reactivity in the solid state, highlighting some recent methodological and theoretical advances. We will also consider some examples of the more exciting and challenging applications of NMR spectroscopy to a range of different materials, including energy materials, biomaterials, geologically relevant materials, and functional solids. Finally, we will conclude by considering where future advances will take this field and the challenges that will remain. By its very nature, a Perspective cannot be a comprehensive review of the area, and readers are also referred to ref 14 (and all articles cited within) for a more complete general overview and detailed discussion of specific areas.

2. BACKGROUND AND BASIC EXPERIMENTS

Solid-state NMR spectra of quadrupolar nuclei are dominated by the interaction between their nuclear electric quadrupole moment, eQ, and the electric field gradient (EFG) at the nucleus.[13] The EFG can be defined in its principal axis system by three components, V_{XX}, V_{YY}, and V_{ZZ}, and is usually described in terms of its magnitude, given by the quadrupolar coupling constant $C_Q = eQV_{ZZ}/h$, and an asymmetry (or shape), $\eta_Q = (V_{XX} - V_{YY})/V_{ZZ}$, such that $0 \leq \eta_Q \leq 1$. The quadrupolar interaction can be very large, with C_Q values of many hundreds of kilohertz to tens or even hundreds of megahertz.[1,2,13] Despite this, in most practically relevant cases the quadrupolar interaction remains smaller than the dominant Zeeman interaction, and its effect upon the nuclear-spin energy levels is described using perturbation theory. Figure 1 shows the perturbation of the Zeeman energy levels caused by the quadrupolar interaction for nuclei with $I = 1$ and $I = {}^3/_2$ and the lifting of the degeneracy of the single-quantum transitions. For the powdered solids most typically studied, different crystallite orientations result in a large anisotropic broadening, although for half-integer spins the central transition (CT) remains relatively sharp and is, in many cases, the only transition observed experimentally.[1,2,13]

The standard technique for improving the resolution in solid-state NMR spectroscopy is MAS,[11] where the sample is rapidly rotated around an axis inclined at an angle of 54.736° with respect to the external magnetic field, as shown in Figure 2a. Samples are packed into rotors of various diameters (Figure 2b), with the maximum possible MAS rate increasing as the rotor diameter decreases. The smallest commercially available rotors, with diameters of 0.75 mm, can be rotated at rates of over 100 kHz. For anisotropic interactions to be removed efficiently, the rotation must be fast (relative to the magnitude of the interaction). This is usually achievable for CSA and many dipolar couplings. However, the magnitude of the quadrupolar interaction is often such that complete averaging is not possible, and the line shape is broken up into a series of spinning sidebands[1,2,14] separated by integer multiples of the spinning rate, as shown by the ^{2}H ($I = 1$) NMR spectra of oxalic acid in Figure 2c,[21] where MAS resolves two resonances corresponding to OD and D_2O species.

In many cases, the magnitude of the quadrupolar interaction is such that the first-order perturbation shown in Figure 1 is not sufficient to describe its effect upon the nuclear energy levels, and higher-order perturbations must be considered.[13] All

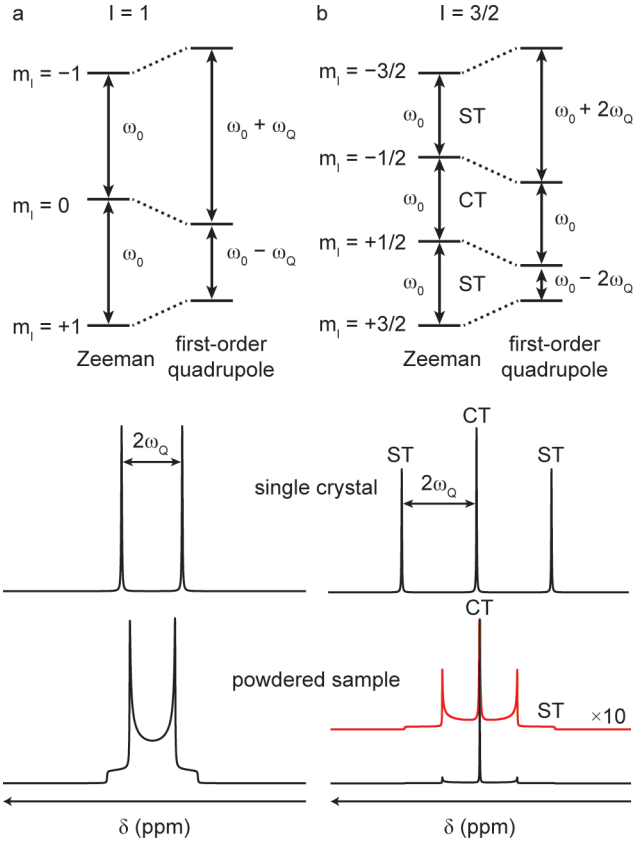

Figure 1. Schematic energy level diagrams showing the effect of the Zeeman and first-order quadrupolar interactions for nuclei with (a) $I = 1$ and (b) $I = {}^3/_2$. For $I = {}^3/_2$, the central transition (CT) is unaffected by the first-order quadrupolar interaction, whereas the satellite transitions (STs) show a significant perturbation. (All of the transitions are affected by the second-order quadrupolar interaction). Also shown are simulations of the resulting single-crystal NMR spectra (now showing $2I$ nondegenerate transitions) and the corresponding powder line shapes.

transitions are affected by the second-order quadrupolar interaction, which has both an isotropic component (with the important result that the resonance position no longer reflects only the chemical shift) and anisotropic components (leading to additional line broadening), as shown by the ^{71}Ga ($I = {}^3/_2$) NMR spectra of $GaPO_4$ berlinite (a simple compound with a single Ga site) in Figure 2d.[22] The second-order broadening increases with C_Q but decreases as the strength of the external magnetic field, B_0, increases, making the use of high magnetic fields particularly beneficial for quadrupolar nuclei. As the second-order quadrupolar interaction has a more complex angular dependence, it is only partially averaged under MAS, and a powder-pattern line shape is still obtained, as can be seen in Figure 2d for $GaPO_4$ berlinite.[22] Simple line shape fitting enables the extraction of the NMR parameters. However, while this is straightforward when only one resonance is present, for materials containing a number of distinct species the line shapes may overlap, as shown in Figure 3a for the ^{23}Na MAS spectrum of $Na_4P_2O_7$ (with four distinct Na species), and it is difficult to extract the relevant information from the complex line shape.[23]

If the magnitude of the quadrupolar interaction is large (a problem exacerbated at low B_0 or for nuclei with low gyromagnetic ratio (γ)), even CT line shapes may be broadened so much that MAS is not able to improve the

dx.doi.org/10.1021/ja504734p | J. Am. Chem. Soc. 2014, 136, 15440−15456

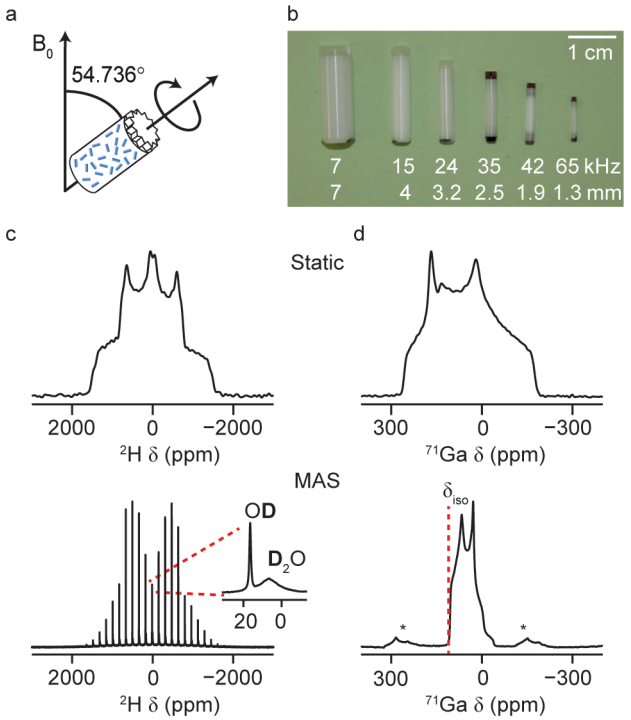

Figure 2. (a) Schematic depiction of the MAS experiment, where a polycrystalline sample is rotated about an axis inclined at an angle of 54.736° with respect to the external magnetic field B_0. (b) Rotors with various outer diameters and the maximum MAS rates that can be achieved with them. (c) Effect of MAS (14 kHz) on the ^{2}H (9.4 T) first-order quadrupolar-broadened line shape of oxalic acid dihydrate ($D_2C_2O_4{\cdot}2D_2O$). The line shape consists of a manifold of spinning sidebands, in each of which resonances from the two distinct ^{2}H sites are resolved. (d) Effect of MAS (14 kHz) on the ^{71}Ga (14.1 T) second-order quadrupolar-broadened CT line shape of $GaPO_4$ berlinite. Under MAS, a powder-pattern line shape is observed (although narrowed in comparison to the static case), but it is shifted from δ_{iso} (shown by the dashed line) by the isotropic quadrupolar shift.

resolution, as sufficiently high rotation rates are not possible. In these cases, it is simplest to obtain a wideline spectrum on a static sample.[24] If the line shapes are very broad, spectra must be acquired in a piecewise manner, with a number of experiments performed at different transmitter frequencies and added together to produce the final spectrum. Recent work by Schurko and co-workers[24−28] has considerably eased the acquisition of wideline spectra through the implementation of pulses (e.g., WURST) that offer more broadband excitation, resulting in improvements in the spectra obtained and reductions in the time taken to acquire them. For wideline experiments, sensitivity is a particular challenge, and many approaches have been used to overcome this, including Carr−Purcell−Meiboom−Gill (CPMG) echo trains[29] and manipulation of the population of the nuclear energy levels using FAM-type[30] pulses, double frequency sweep (DFS) pulses,[31] or shaped hyperbolic secant (HS) pulses.[14,32] Most of the approaches used are equally applicable to rotating samples and can be employed in conventional MAS experiments. References 33 and 34 provide more detail in this area.

The combination of broadband pulses and sensitivity improvements, coupled with the recent availability of high magnetic fields, has certainly resulted in a step change in the quality of wideline spectra that can be obtained and has expanded the range of materials that can be studied, and this approach has recently been applied to, e.g., ^{35}Cl NMR of organometallic complexes,[35] ^{25}Mg NMR in minerals,[36] ^{87}Sr NMR of carboxylates,[37] NMR of ^{115}In complexes[38] and inorganic ^{135}Ba compounds,[39] ^{79}Br and ^{127}I NMR,[18] and the acquisition of ^{14}N (I = 1) NMR spectra.[40] While interesting correlations of the NMR parameters with structural features such as the nature of ligand binding[35] or the strength of halogen bonds[41] have been observed, applications do seem restricted to cases where the number of overlapped line shapes is very small and other interactions (such as dipolar couplings) do not significantly affect the spectra. In many cases, removal of the broadening and resolution of distinct sites will be required before structural information can be obtained.

3. THE QUEST FOR RESOLUTION

The broadening in the NMR spectra of quadrupolar nuclei limits both sensitivity and resolution and severely hampers the extraction of site-specific structural information. Perhaps the most enduring aim in solid-state NMR spectroscopy of quadrupolar nuclei over the last few decades, therefore, has been the complete removal of the quadrupolar broadening and the acquisition of high-resolution (isotropic) spectra, and although most of the major developments in this area are less recent, this subject has had such an impact on the history of NMR spectroscopy of quadrupolar nuclei that a brief review of the methods now used is warranted.

The orientational dependence of the second-order quadrupolar broadening is more complex than those of CSA and dipolar couplings (or the first-order quadrupolar interaction) and cannot be removed by spinning around a single angle alone. The first approaches to solving this problem, developed in the late 1980s, were composite sample rotation techniques, i.e., involving rotation of the sample around two different angles, simultaneously in the case of double rotation (DOR)[42] and sequentially for dynamic angle spinning (DAS).[43] Conceptually, DOR is easier to understand, with two rotors used, one inside the other. Each spins at a different angle (54.74° or 30.56°) to average the two different anisotropic components of the broadening. In DAS, the sample is sequentially rotated around two different angles (for different times) in a two-dimensional experiment,[42] with times and angles chosen such that the quadrupolar broadening is refocused. Further information on DOR and DAS is provided in ref 14.

The study of quadrupolar nuclei in the solid state was revolutionized in 1995 by the introduction of the multiple-quantum (MQ) MAS experiment.[44] Unlike DAS and DOR, MQMAS uses sample rotation around a single angle (i.e., 54.736°, thereby additionally removing CSA and dipolar interactions) and thus can be performed using a conventional probehead. Removal of the second-order quadrupolar interaction is achieved within a two-dimensional experiment where multiple-quantum (e.g., $m_I = +^3/_2 \leftrightarrow m_I = -^3/_2$) coherences are correlated with CT coherences. The result is shown in Figure 3b, where the four distinct ^{23}Na species in $Na_4P_2O_7$ can now be resolved in the ^{23}Na MQMAS spectrum.[23] Cross sections enable the NMR parameters for each site to be determined individually, as shown in Figure 3c. A more detailed discussion of MQMAS can be found in refs 14, 45, and 46. A conceptually similar experiment, termed STMAS, that uses the correlation of single-quantum satellite transitions (ST) rather than multiple-quantum transitions was introduced in 2000 by Gan[47] as an

dx.doi.org/10.1021/ja504734p | J. Am. Chem. Soc. 2014, 136, 15440−15456

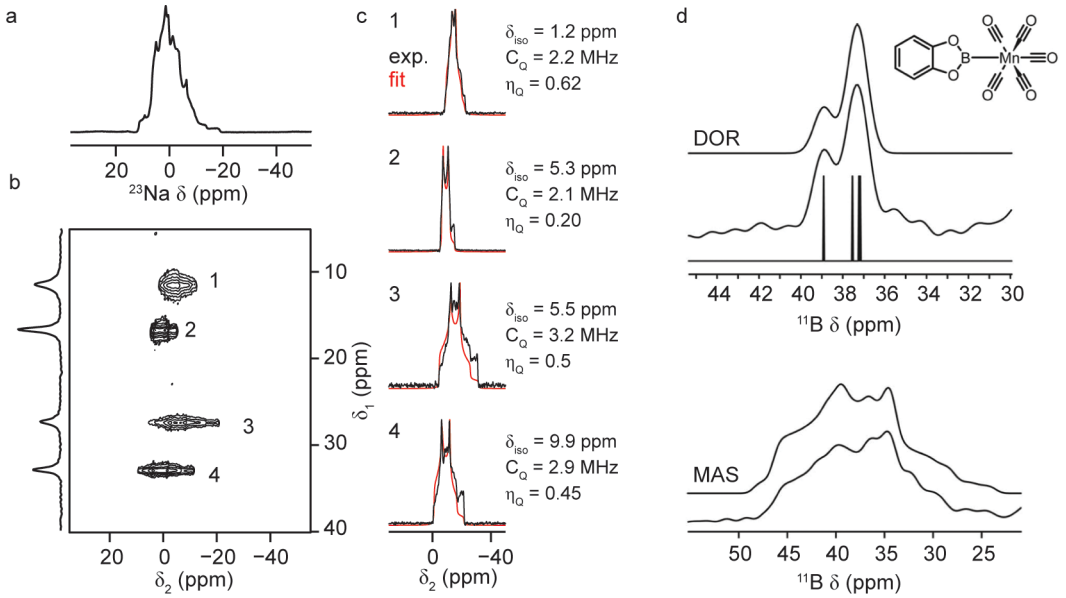

Figure 3. ^{23}Na (14 kHz, 14.1 T) (a) MAS and (b) triple-quantum MAS spectra of $Na_4P_2O_7$. (c) Cross sections (extracted parallel to δ_2) for each of the four Na species; the corresponding fits with the relevant NMR parameters are also given. (d) (top) ^{11}B DOR spectra (experiment and two simulations) and (bottom) MAS spectra (experiment and simulation) of manganese catecholboryl pentacarbonyl. Reprinted with permission from ref 52. Copyright 2013 AIP Publishing LLC.

Table 1. Properties of Selected Quadrupolar Nuclei

nucleus	I	N/%	$\gamma/(10^7$ rad s^{-1} T$^{-1})$	ν_0/MHz[a]	receptivity[b]	Q/fm^2
^{2}H	1	0.01	4.107	92.12	1.11×10^{-6}	0.286
^{6}Li	1	7.59	3.937	88.32	6.45×10^{-4}	−0.0808
^{7}Li	$^{3}/_{2}$	92.41	10.398	233.23	2.71×10^{-1}	−4.01
^{10}B	3	19.9	2.875	64.48	3.95×10^{-3}	8.459
^{11}B	$^{3}/_{2}$	80.1	8.585	192.55	1.32×10^{-1}	4.059
^{14}N	1	99.64	1.934	43.38	1.00×10^{-3}	2.044
^{17}O	$^{5}/_{2}$	0.04	−3.628	81.36	1.10×10^{-5}	−2.558
^{23}Na	$^{3}/_{2}$	100.00	7.081	158.75	9.26×10^{-2}	10.4
^{25}Mg	$^{5}/_{2}$	10.00	−1.639	36.74	2.68×10^{-4}	19.94
^{27}Al	$^{5}/_{2}$	100.00	6.976	156.38	2.06×10^{-1}	14.66
^{33}S	$^{3}/_{2}$	0.75	2.056	46.07	1.70×10^{-5}	−6.78
^{35}Cl	$^{3}/_{2}$	75.76	2.624	58.80	3.56×10^{-3}	−8.165
^{37}Cl	$^{3}/_{2}$	24.24	2.184	48.95	6.58×10^{-4}	−6.435
^{39}K	$^{3}/_{2}$	93.26	1.250	28.00	4.74×10^{-4}	5.85
^{43}Ca	$^{7}/_{2}$	0.14	−1.80	40.39	8.64×10^{-6}	−4.08
^{45}Sc	$^{7}/_{2}$	100.00	6.51	145.78	3.01×10^{-1}	−22.0
^{47}Ti	$^{5}/_{2}$	7.44	−1.51	33.83	1.56×10^{-4}	30.2
^{49}Ti	$^{7}/_{2}$	5.41	−1.51	33.84	2.04×10^{-4}	24.7
^{51}V	$^{7}/_{2}$	99.75	7.05	157.85	3.81×10^{-1}	−5.2
^{55}Mn	$^{5}/_{2}$	100.00	6.65	148.77	1.78×10^{-1}	33
^{59}Co	$^{7}/_{2}$	100.00	6.33	142.39	2.81×10^{-1}	42
^{67}Zn	$^{5}/_{2}$	4.10	1.68	37.55	1.17×10^{-4}	15.0
^{69}Ga	$^{3}/_{2}$	60.11	6.44	144.04	4.16×10^{-2}	17.1
^{71}Ga	$^{3}/_{2}$	39.89	8.18	183.02	5.66×10^{-2}	10.7
^{79}Br	$^{3}/_{2}$	50.69	6.73	150.37	4.00×10^{-2}	30.5
^{81}Br	$^{3}/_{2}$	49.31	7.25	162.07	4.86×10^{-2}	25.4
^{87}Rb	$^{3}/_{2}$	27.83	8.79	196.37	4.88×10^{-2}	13.35
^{91}Zr	$^{5}/_{2}$	11.22	−2.50	55.79	1.05×10^{-3}	−17.6
^{93}Nb	$^{9}/_{2}$	100.00	6.57	146.89	4.84×10^{-1}	−32
^{133}Cs	$^{7}/_{2}$	100.00	3.53	78.71	4.74×10^{-2}	−0.343
^{139}La	$^{7}/_{2}$	99.91	3.81	84.77	5.91×10^{-2}	20

[a]Larmor frequency at 14.1 T. [b]Quoted relative to ^{1}H.

dx.doi.org/10.1021/ja504734p | J. Am. Chem. Soc. 2014, 136, 15440−15456

alternative approach. Its implementation is more challenging than that of MQMAS (with the need for very accurate adjustment of the spinning angle (to ±0.002°), a stable spinning rate, and accurate pulse timings), but it typically offers a significant sensitivity advantage over MQMAS (in many cases by factors of between 4 and 8). Further information on STMAS is provided in refs 14 and 48.

A pertinent question for the solid-state chemist is which of these established methods to choose? The literature shows that the most widely applied technique is MQMAS, which has enabled site resolution and extraction of structural information in many different chemical systems.[45,46] One obvious reason for this popularity is the need for only a conventional MAS probehead, whereas both DOR and DAS require dedicated hardware, which has ensured that they have remained largely within the realm of the specialist. The easy implementation of MQMAS is offset somewhat by its inherently poor sensitivity. Much effort has been focused on improving this in recent years, and good results have been obtained using the FAM, DFS, and HS pulses discussed earlier, while the soft pulse added mixing (SPAM) approach provides sensitivity enhancement at relatively little additional cost.[6,30−32,49,50] Despite these advances, the poor efficiency of MQMAS can remain a problem for challenging samples and nuclei with inherently low sensitivity. While STMAS also requires only conventional hardware (and has much greater sensitivity), the stricter requirements on its implementation appear to have restricted its use, with its greatest successes achieved when the sensitivity is limited (i.e., small sample volumes and nuclei with low natural abundance or low γ).[48] In recent years, improved hardware has eased the implementation of STMAS, and although it perhaps is not fulfilling its true potential at present, it should become more popular in the future.

Recent hardware advances have, however, also seen a resurgence of interest in DOR, although the size of the outer rotor does still restrict the MAS rates that can be used, producing a range of spinning sidebands that can complicate spectral analysis. Impressive recent work has used DOR to investigate dipolar and J couplings between quadrupolar spins,[51−53] providing not only information on the fundamental nature, presence, and magnitude of higher-order interactions[54] (of interest to the specialist) but also important structural information of interest to the chemist. Figure 3d shows the ^{11}B DOR (top) and MAS (bottom) spectra of manganese catecholboryl pentacarbonyl. The coupling patterns revealed by DOR enabled information on the ^{55}Mn quadrupolar interaction to be extracted, enabling the observation that the interaction of Mn with the carbonyl ligands is stronger than that with the catecholboryl ligand.[52]

The desire to remove the quadrupolar broadening and acquire high-resolution spectra has driven much research over the past few decades. However, with the progress made in recent years, it is now possible not only to achieve this almost routinely but also to combine experiments such as MQMAS and STMAS with the magnetization transfer experiments commonly used in spin $I = {}^1/_2$ NMR studies, enabling access to the full panoply of information that NMR spectroscopy can provide.

4. COMMONLY STUDIED QUADRUPOLAR NUCLEI

The ease with which an NMR spectrum can be acquired is determined by a number of parameters including the natural abundance (N), spin quantum number (I), and gyromagnetic ratio (γ) of the nucleus. These are typically combined into a quantity called the receptivity, given by $\gamma^3NI(I + 1)$, which is usually quoted relative to ^{1}H. However, for quadrupolar nuclei another important factor is the magnitude of the quadrupolar broadening of the spectral lines. Although for any specific material this depends upon the EFG and the Sternheimer antishielding factor,[55] the magnitude of the nuclear quadrupole moment is an important consideration. Table 1 gives the nuclear properties for some of the more commonly studied quadrupolar nuclei, and Figure 4 shows a plot of the receptivities, gyromagnetic ratios, and quadrupole moments of a range of isotopes.[2,14]

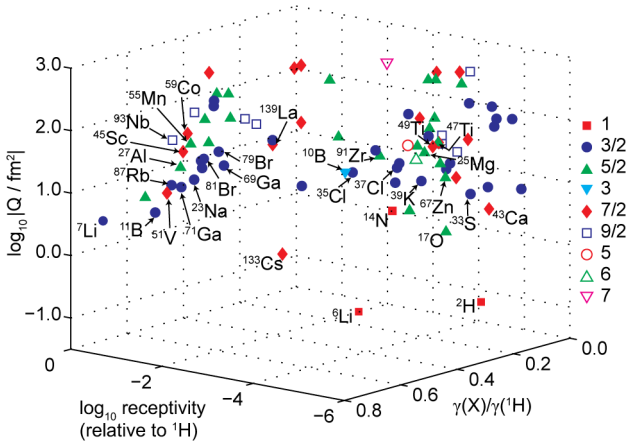

Figure 4. Three-dimensional plot showing the receptivities ($\log_{10}$ $\gamma^3NI(I + 1)$, quoted relative to ^{1}H), gyromagnetic ratios (γ, quoted relative to ^{1}H), and quadrupole moments ($\log_{10}$ |Q|) for quadrupolar nuclides. Commonly studied nuclei (i.e., those given in Table 1) are marked.

Commonly studied nuclei include those with reasonable natural abundance and small to medium quadrupolar coupling (e.g., $^{6/7}$Li, ^{11}B, ^{23}Na, ^{27}Al, ^{45}Sc, etc., as shown in Figure 4), while for nuclei with low natural abundance (e.g., ^{17}O) isotopic enrichment often has to be employed. For nuclei with low γ, such as ^{39}K and ^{25}Mg (see Figure 4), high magnetic field and the sensitivity enhancement techniques discussed above are usually required. Fast MAS is usually needed for nuclei exhibiting larger quadrupolar interactions, such as $^{69/71}$Ga and ^{93}Nb, while for species where the quadrupolar broadening is often much larger than available MAS rates (e.g., $^{35/37}$Cl, $^{79/81}$Br, ^{127}I, ^{91}Zr, ^{87}Sr) the wideline approaches discussed above are preferred. Although NMR spectroscopy of nuclei with integer spin is typically quite different from that of nuclei with half-integer spin (because of the lack of a narrow CT) and could indeed form the basis for an entire review or Perspective in itself, it is worth mentioning the two such nuclei most commonly studied here: ^{2}H and ^{14}N.[14,56,57] Spectral acquisition is restricted to systems and species with smaller quadrupolar couplings (many ^{2}H species and ^{14}N in symmetrical environments) for MAS experiments, while wideline spectra of static samples are acquired for materials exhibiting larger C_Q.

5. CHEMICAL STRUCTURE AND DISORDER

With diffraction firmly established as the method of choice among most chemists for the characterization of solids, it is worth considering the information that NMR spectroscopy can provide and where its relative strengths lie. As nuclear spins are

dx.doi.org/10.1021/ja504734p | J. Am. Chem. Soc. 2014, 136, 15440−15456

affected by a variety of structure-dependent interactions, NMR spectroscopy is able to provide detailed insight into the atomic-scale environment within a solid. On a basic level, the number of resonances and their relative intensities reveal the number and proportions of distinct species in the material and thus can confirm (or disprove!) the proposed symmetry or space group. Although less straightforward than for $I = {}^1/_2$ systems, this information can be obtained from many MAS spectra of quadrupolar nuclei, as shown in Figure 5a, where the ^{23}Na

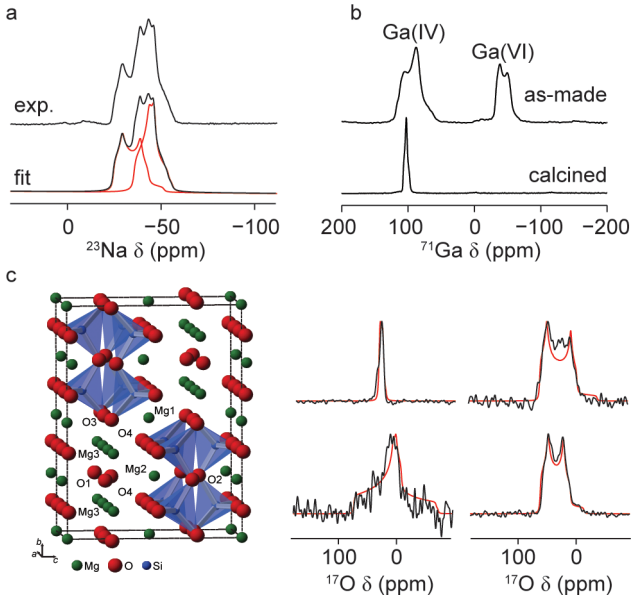

Figure 5. (a) ^{23}Na (12.5 kHz, 9.4 T) MAS NMR spectrum of $Na_2[(VO)_2(HPO_4)_2C_2O_4]\cdot 2H_2O$ and the corresponding simulated fit showing two overlapping resonances, confirming the space group as $P2_1$ rather than $P2_1/m$. Adapted from ref 58. Copyright 2006 American Chemical Society. (b) ^{71}Ga (25−30 kHz, 20.0 T) MAS NMR spectrum of as-made and calcined GaPO-34, showing the change in the coordination number of the framework species upon calcination. Adapted from ref 22. Copyright 2012 American Chemical Society. (c) Structure of wadsleyite, β-Mg_2SiO_4, and cross sections (extracted from STMAS spectra) and line shapes generated using parameters calculated by DFT for each of the four O species. Adapted from ref 67 with permission from the PCCP Owner Societies.

NMR spectrum of a novel vanadyl oxalatophosphate, $Na_2[(VO)_2(HPO_4)_2C_2O_4]\cdot 2H_2O$, is able to distinguish between two proposed space groups, $P2_1/m$ and $P2_1$, obtained from refinements of the diffraction measurements.[58] The presence of two overlapping quadrupolar line shapes supports a space group of $P2_1$ rather than $P2_1/m$, where only a single distinct Na species would be expected. Spectroscopy can also identify minor impurities in materials (or those more difficult to distinguish by diffraction) that might have important effects upon the properties.[59,60] More generally, the magnitudes of various NMR parameters can provide structural information, and many authors have attempted to determine (with varied success) the dependence of the NMR parameters upon the local geometry for a range of quadrupolar nuclei.[2] The coordination number of a species can have a significant effect upon δ_{iso}, as illustrated by the ^{71}Ga ($I = {}^3/_2$) spectra of the as-made and calcined GaPO-34 microporous frameworks shown in Figure 5b.[22] In the as-made sample, F^- anions bridge two Ga1 atoms, creating both four- (Ga2 and Ga3) and six-coordinate (Ga1) gallium. Upon calcination, a purely tetrahedral framework is produced, as shown by the change in chemical shift, while the symmetry change from $P\bar{1}$ to $R\bar{3}$ is reflected in the presence of just one quadrupolar line shape. Other well-known examples include the significant difference in ^{11}B C_Q values for trigonal (2−2.8 MHz) and tetrahedral (0−0.6 MHz) boron[2] and the dependence of the ^{17}O C_Q upon the covalency of the X−O bond, an observation that allows bridging (e.g., Si−O−Si) and nonbridging (e.g., Si−O−Mg) species to be distinguished in minerals and glasses.[19] Also commonly exploited in the study of biological and organic materials is the dependence of ^{2}H NMR parameters (both C_Q and δ_{iso}) on the geometry (i.e., both distance and angle) of hydrogen bonds.[61]

Once a spectrum has been obtained, the subsequent aim is to extract information on the type of species present (and how they might change with variation, e.g., in synthetic approach, in composition, over time, or after reaction). Authors have previously sought to exploit the range of empirical relationships between NMR parameters and geometry to propose tentative spectral assignments.[2] However, considerable care must be taken, as many different aspects of a structure can affect the NMR parameters. A classic example is the ^{27}Al NMR spectrum of andalusite, Al_2SiO_5, which contains two distinct Al sites corresponding to five- and six-coordinate Al. Two resonances are observed in the spectrum, with C_Q values of 5.8 and 15.3 MHz, respectively.[2,62] However, the latter results not from the five-coordinate Al as expected, but from the six-coordinate Al species because of a significant distortion of the coordination environment. In recent years, an alternative approach has been used to aid spectral understanding, exploiting the developments in the calculation of NMR parameters from first principles. Although such calculations have been used in conjunction with experiment in various areas of chemistry for many years, the need to approximate a solid as a cluster (centered on the atom of interest and with remote bonds terminated, typically by H) had limited the influence of computation in solid-state NMR spectroscopy. Interest in this area has been revitalized in recent years by the introduction of codes exploiting periodic boundary conditions to recreate the extended three-dimensional structure of a solid, most of which use density functional theory (DFT), a theoretical framework favored for its cost efficiency and accuracy.[63] The impact these methods have had on the experimental NMR community in particular has been significant, as evidenced by recent reviews.[64−66] Calculations play a key role in interpreting and assigning NMR spectra, as shown in Figure 5c, where quadrupolar-broadened ^{17}O NMR line shapes (extracted from an STMAS spectrum) of the four distinct ^{17}O species in wadsleyite, β-Mg_2SiO_4, are compared to those predicted using DFT calculations.[8,67] The calculations not only enabled assignment of the four oxygen species but also verified the unexpectedly high experimental C_Q values[68] for the nonbridging species O3 and O4 (4.4 and 3.8 MHz, respectively), which are more typical of those expected for bridging oxygen atoms.

Although in some cases calculations are used to support and verify experimental measurements, their ultimate impact will result from the insight they provide for materials where the structure is not known or not fully defined, enabling the validity of potential structural models to be evaluated by comparing calculated and experimental NMR parameters. Calculations can also play a significant role in "NMR crystallography",[69] where the combination of information from diffraction and NMR spectroscopy is used to provide quantitative structural detail

dx.doi.org/10.1021/ja504734p | J. Am. Chem. Soc. 2014, 136, 15440−15456

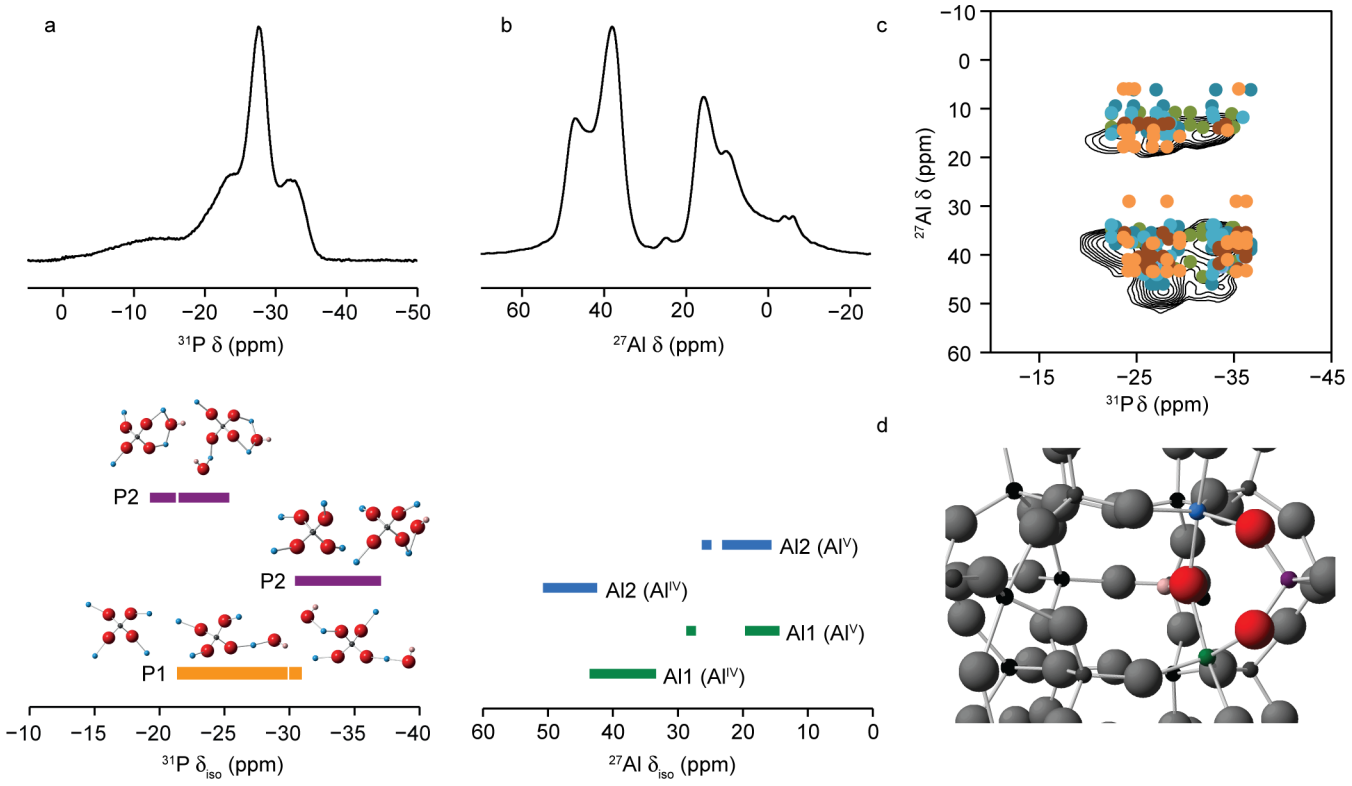

Figure 6. NMR spectra of as-made STA-2. (a, b) MAS NMR spectra and plots of chemical shifts arising from DFT calculations for possible structural models with differing positions of the charge-balancing hydroxyls for (a) ^{31}P (14 kHz, 14.1 T) and (b) ^{27}Al (14 kHz, 14.1 T). (c) Two-dimensional ^{27}Al/^{31}P (12.5 kHz, 20.0 T) HETCOR spectrum and (overlaid) cross-peak positions from DFT calculations. (d) Schematic of framework-bound hydroxyl anion in a cancrinite cage. Good agreement with experiment is obtained only for models where the hydroxyls are in different cancrinite cages and do not share a double four-membered ring. Adapted from ref 92, published by The Royal Society of Chemistry.

that cannot be obtained from either method alone. The addition of computation (sometimes then termed "SMARTER crystallography") provides a link between the two experimental approaches. An excellent example of this is the recent work of Martineau et al.,[70] in which a structural model for a fluorinated inorganic-organic hybrid, $Zn_3Al_2F_{12}[HAmTAZ]_6$ (AmTAZ = 3-aminotriazole), was proposed using unit cell dimensions and a number of possible space groups (from diffraction) and the number and proportion of distinct species and their coordination environments (from ^{27}Al, ^{67}Zn, ^{19}F, ^{1}H, ^{15}N, and ^{13}C NMR). Possible models were then optimized and ultimately validated using DFT calculations. Although perhaps not yet routine, the combination of periodic calculations alongside experiment is now used frequently for simple systems, and the study of more complex materials is beginning to be tackled with more advanced computational approaches. This has certainly been one of the most successful areas of recent development and will undoubtedly have a wide and lasting impact on the field in the coming years.

Although information can be obtained from conventional NMR spectra, for detailed structural insight it is necessary to understand how the atoms in a structure are arranged in relation to each other. This can be achieved by probing the interactions between spins, either through space (for dipolar interactions) or via covalent bonds (for J coupling). Recently there have been significant developments in the application of two-dimensional correlation experiments, previously used only for $I = {}^1/_2$ nuclei, to quadrupolar spins. Both heteronuclear and homonuclear experiments are known, although the former are typically easier both to implement and to interpret,[14,20,71] and in many cases experiments are combined with MQMAS to improve the resolution for the quadrupolar spin(s).[14,71] The transfer of magnetization through heteronuclear J coupling is common, with, e.g., ^{27}Al/^{31}P, ^{71}Ga/^{31}P, and ^{27}Al/^{17}O experiments all being utilized.[71−75] However, the relatively small J couplings for many quadrupolar nuclei have resulted in the greater development of approaches that exploit the (larger) dipolar interaction. A commonly used approach for transferring magnetization between spin $I = {}^1/_2$ nuclei via dipolar coupling is cross-polarization (CP). However, CP dynamics are significantly more complicated for quadrupolar nuclei,[76,77] as the efficiency depends upon the radiofrequency (rf) field strength, the quadrupolar coupling, and the spinning rate.[78,79] Alternative approaches utilized in recent years involve the use of trains of rf pulses to recouple (i.e., reintroduce) the dipolar interaction in experiments initially designed to utilize J couplings.[6,71,80−84] While a common complaint from the nonspecialist is that the vast number of possible experiments (and their often inexplicable acronyms) is confusing, essentially all of the experiments are similar, with the transfer of magnetization from one type of spin to another and a cross-peak in the spectrum indicating the presence (and sometimes magnitude) of the interaction that they share. However, advances continue to be made, with one of the more recent being the introduction of a suite of methods for acquiring (indirectly) ^{14}N MAS spectra (see later for a more detailed discussion).[85−87] In general, this is an important area of considerable current development, and further progress over the next few years will ease both the choice (once the most efficient and more robust methods have been established) and

dx.doi.org/10.1021/ja504734p | J. Am. Chem. Soc. 2014, 136, 15440−15456

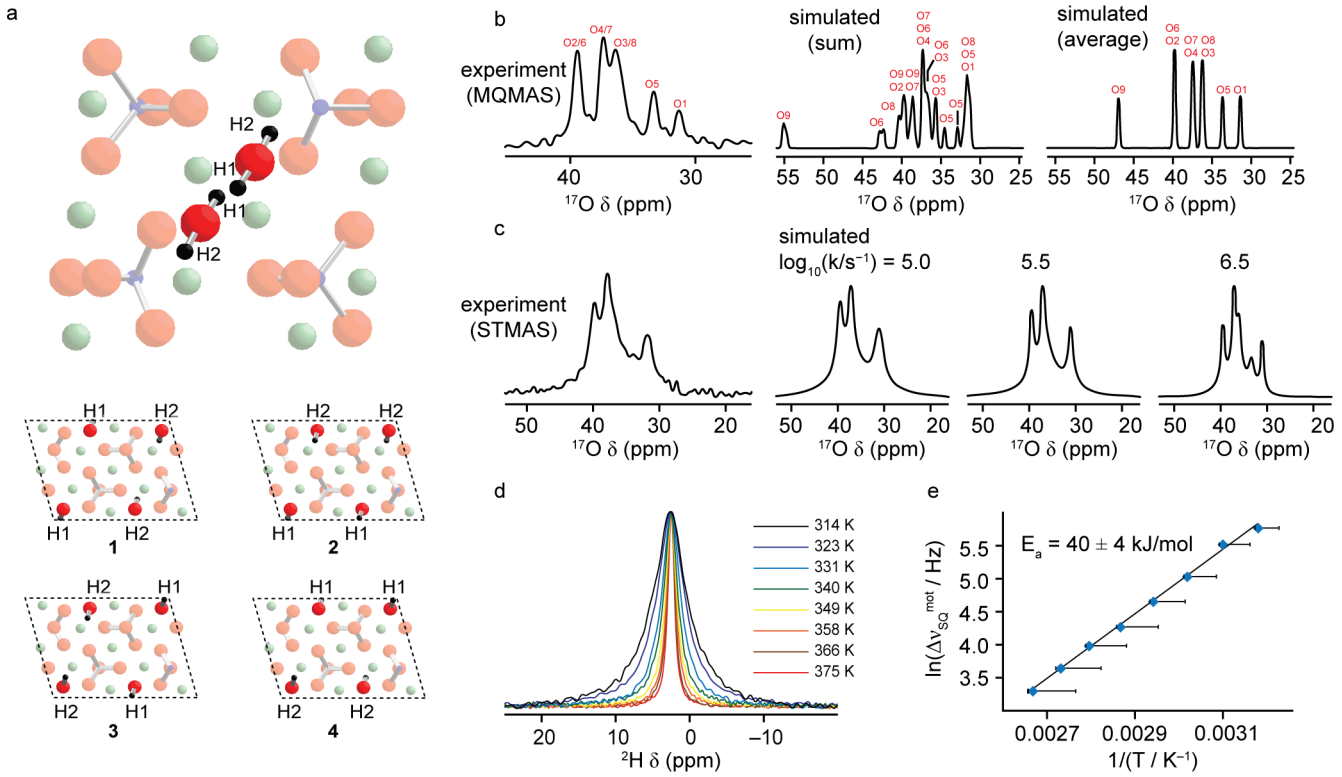

Figure 7. (a) The two possible proton positions H1 and H2 associated with each hydroxyl group in clinohumite, $4Mg_2SiO_4{\cdot}Mg(OH)_2$, and the models used in the DFT calculations. (b, c) ^{17}O (8 kHz, 9.4 T) MQMAS and STMAS spectra, respectively, of clinohumite. Also shown in (b) and (c) are spectra resulting from the summation and averaging of simulated ^{17}O isotropic spectra calculated for different arrangements of the hydroxyl groups. In (c), STMAS spectra are simulated using the calculated NMR parameters for the different structural models and an additional line broadening determined using a simple model for motional broadening. (d) Variable-temperature ^2H (10 kHz, 9.4 T) MAS NMR spectra of deuterated clinohumite and (e) the resulting Arrhenius plot to extract the activation energy. Adapted from ref 103. Copyright 2008 American Chemical Society. Adapted from ref 104 with permission from the PCCP Owner Societies.

implementation of these methods for a specific system for the general chemist.

For materials exhibiting a deviation from the periodicity associated with the solid state, i.e., those with compositional or positional disorder, structure solution is considerably more challenging, and NMR spectroscopy provides a vital complementary tool to diffraction for the chemist. Disorder can give rise to many effects in the NMR spectrum, including additional or overlapped resonances and broadening of the spectral lines. For quadrupolar nuclei, distributions in both the chemical shift and quadrupolar coupling constant can result, leading to additional broadening and a characteristic "tail" to low frequency on the spectral lines. These line shapes (and those in corresponding two-dimensional spectra) can be fitted using a Czjzek model to extract information on the distributions present.[88] This broadening can make it more difficult to resolve overlapping contributions even when MQMAS is used, and information from next-nearest neighbor (NNN) atoms can be more difficult to obtain. This can be overcome to some extent by combining experiments with DFT calculations for a series of structural models where the local environment of an atom is varied and the calculated NMR parameters are then compared with experiment.[66,89−95] Some recent examples (see also later sections) include ^{27}Al NMR spectroscopy and DFT calculations to probe the Al/Si cation disorder in gehlenite, $Ca_2Al_2SiO_7$,[91] where contributions from the seven Al local environments can be distinguished, and $^{27}Al/^{31}P$ NMR spectroscopy to investigate anion disorder in the AlPO framework STA-2.[92] For this latter case, as shown in Figure 6, comparison of a range of ^{27}Al and ^{31}P NMR spectra with the NMR parameters calculated for models with differing hydroxyl positions was able to show that hydroxyls bridge Al1 and Al2 in the cancrinite cages but that two hydroxyls do not occupy the same cage simultaneously.[90]

6. DYNAMICS AND CHEMICAL REACTIVITY

NMR spectroscopy has proven to be a useful probe of dynamics in the solid state because of its sensitivity to motion on time scales that vary over many orders of magnitude. This arises from a modulation of the resonance frequency caused by motion either of an atom itself or of atom(s) in the local surroundings. Different motional time scales can be investigated, with fast motion (10^7 to 10^{11} s^{-1}) probed by changes in relaxation (not discussed in detail here), slow motions (10^3 to 10^{-1} s^{-1}) by exchange experiments, and rates intermediate to these extremes by changes to the spectral resonances. For quadrupolar nuclei, motion modulates the EFG tensor, and therefore, the spectra are sensitive to time scales determined by the inverse of the line width, typically 10^7 to 10^4 s^{-1} for resonances broadened by the first-order quadrupolar interaction and 10^5 to 10^3 s^{-1} for CT line shapes subject to second-order quadrupolar broadening.[96]

One of the most commonly exploited quadrupolar nuclei for studying dynamics is ^2H ($I = 1$), with typical line widths (for static samples) of 1−200 kHz.[57,96,97] Furthermore, the ability to perform selective deuteratation provides site-specific motional information. Changes in the spectral line shape as a function of

dx.doi.org/10.1021/ja504734p | J. Am. Chem. Soc. 2014, 136, 15440−15456

temperature provide information on the geometry of the dynamic process and its rate, typically by comparison of experimental and simulated line shapes.[97] Wideline experiments have also recently been demonstrated for ^{14}N in elegant work by Schurko and O'Dell and offer similar potential for the future.[40,56,96] In addition to improving resolution and sensitivity, the use of MAS is also able to extend the time scales that can be probed by ^{2}H NMR spectroscopy, with the width of the sidebands being affected by the interference of motion with the averaging of the quadrupolar interaction by MAS.[21,96] In contrast to line shape analysis, where the geometry of the motional process must be known, model-independent information (on the rate or activation energy) can be obtained from the variation of the line width with temperature for each resolved resonance.[98,99]

For nuclei with half-integer spin quantum number, only the CT is typically observed. The shape and width of this second-order-broadened line shape is also sensitive to dynamics (at rates comparable to the magnitude of the interaction).[96] While comparison of experimental and simulated line shapes is, in principle, able to determine the type and rate of motion, the overlap of line shapes in an MAS spectrum hinders the extraction of accurate and site-specific information. However, if resonances are reasonably well resolved, variable-temperature MAS experiments can provide information, and ^{17}O NMR spectroscopy in particular has been exploited in this manner by a number of authors.[96] An elegant example is the work of Hampson et al.,[100] who used two-dimensional ^{17}O exchange spectroscopy (EXSY) experiments to distinguish the motional model and time scale (10 s^{-1}) for the hopping of the WO_4 groups in ZrW_2O_8. If multiple sites are overlapped in an MAS spectrum, high-resolution MQMAS or STMAS experiments may be used. As described above, MQMAS uses transitions that are not affected by the first-order quadrupolar interaction and thus would only be affected by slower motion. In contrast, the STs are affected by the much larger first-order quadrupolar interaction, and motion on the microsecond time scale results in significant broadening of the resonances. This was first demonstrated for a microporous phosphate framework, AlPO-14, where broadening of the ^{27}Al STMAS spectrum was observed as a result of motion of the template (isopropylammonium) within the pores of the material.[48,101]

The combination of DFT calculations and experiment can be particularly powerful in the study of dynamics. One example of this is the recent investigation of clinohumite, $4Mg_2SiO_4 \cdot Mg(OH)_2$,[8,102−105] which exhibits two possible hydroxyl proton positions, H1 and H2 (see Figure 7a), each of which has a fractional occupancy (from diffraction) of 0.5. Figure 7b shows that the ^{17}O MQMAS spectrum simulated by summing calculated spectra for different structural models is in poor agreement with experiment. However, there is much better agreement when the calculated ^{17}O NMR parameters are averaged prior to simulation, suggesting that there is dynamic rather than static disorder of the hydroxyl groups.[103] This is confirmed in Figure 7c, where the isotropic experimental ^{17}O STMAS spectra show significant broadening of some of the resonances as a result of hydroxyl dynamics and confirm that $\log_{10} k = 5.5$.[101] The temperature-dependent MAS line width enables the determination of an activation energy of 40 ± 4 kJ mol^{-1} for H1/H2 exchange (Figure 7d,e).[104]

The sensitivity of NMR spectroscopy to local structure and to dynamics makes it a convenient tool for following physical and chemical transformations. These can be as simple as (de)hydration, which is often apparent from the change in coordination number of nuclei such as ^{27}Al and ^{71}Ga or, alternatively, more major changes to the NMR spectrum, as observed for some metal-organic framework (MOF) materials.[3,5,9] NMR spectroscopy can also be used to follow phase transitions as a function of temperature or to probe the host-guest interactions in materials where small molecules can be chemisorbed or physisorbed. Chemical reactions can also be followed using NMR spectroscopy, which allows the nature of the products and the reaction rate to be probed. Transformations can be followed ex situ (i.e., carrying out reactions under laboratory conditions) by quenching at a variety of times and analyzing the products. Of considerably more use, however, are in situ studies, which have the added advantage of enabling the detection of transient species. Simple (de)hydration processes can be easily followed, and in some cases occur inadvertently, by means of the frictional heating resulting from either MAS or decoupling. Such a reversible phase transition was observed for AlPO-53(A),[106] which dehydrated in the rotor to produce the related phase JDF-2, a change that was immediately apparent from the ^{27}Al MAS NMR spectra. For more complex reactions, in situ NMR can be challenging both from a practical point of view (with the need to reproduce conditions, i.e., temperature, pressure, and reactant flow of a reaction, when the sample is spinning) and, for quadrupolar nuclei, from a spectroscopic point of view, with the presence of the quadrupolar broadening. For more ambitious reactions, in situ experiments are more usually performed on static samples using hardware specially adapted to enable the reaction conditions to be reproduced as closely as possible (see below for examples). Although these experiments are an exciting area (particularly for those interested in catalysis and small-molecule storage), they remain practically challenging, and considerable advances are required before they can be considered in any sense routine. They do, however, perhaps offer one of the more interesting avenues for future development, as dynamics and reactions are often difficult to study in real time using other techniques.

7. RECENT APPLICATIONS OF SOLID-STATE NMR SPECTROSCOPY OF QUADRUPOLAR NUCLEI

Solid-state NMR spectroscopy of quadrupolar nuclei has been widely applied to a range of problems in areas as diverse as chemistry, biology, geology, and materials science. While a complete review is of course not practical in the context of a Perspective, below we highlight some recent applications in a few areas of current interest to show what is presently possible. The reader is referred to the literature for more detailed reviews.[3,8−10,14−20]

Quadrupolar NMR Spectroscopy of Energy Materials. Among the major challenges facing the world today are the growing threats from global warming, geopolitics, and the finite amount of extractable fossil fuel reserves. It is anticipated that the world's energy systems will have to undergo a radical change in the near future, resulting in a pressing search for new energy materials that are efficient, clean, and cost-effective both to produce and to operate. Solid-state NMR spectroscopy is ideally suited not only for the study of the local structure of such materials but also for the investigation of the dynamic and electrochemical processes that occur.[14,107−109] Research to date has focused primarily on lithium battery materials and oxide ion conductors, with $^{6/7}$Li and ^{17}O NMR attracting considerable recent attention.[14,107−109] However, the experimental chal-

dx.doi.org/10.1021/ja504734p | J. Am. Chem. Soc. 2014, 136, 15440−15456

lenges posed here do not necessarily result from the quadrupolar nature of these nuclides, but instead arise from the need to understand the processes and structural changes that occur under operating conditions (i.e., in situ) to be of real relevance.

Many investigations of energy materials have exploited $^{6/7}$Li NMR spectroscopy because of the widespread use of lithium ion battery technology. Spectral acquisition is eased by small quadrupolar couplings and high sensitivity, and although diamagnetic materials exhibit a very small chemical shift range (typically a few ppm), the chemical shifts for Li in paramagnetic systems can be quite significant, often in the range of 1600 ppm.[2,107−109] Despite the success of lithium ion batteries, the toxicity and cost of the most commonly used cathode material, $LiCoO_2$, has prompted researchers to find viable alternatives. One promising series of materials are the layered lithium cobalt nickel manganese oxides, i.e., $LiMO_2$ (where M = Ni, Mn, Co). Using ^{6}Li MAS NMR spectroscopy, Yoon et al.[110] were able to demonstrate that lithium was found in both the transition-metal and lithium layers (the former demonstrated by the significant shifts resulting from the Ni^{2+} and Mn^{4+} neighbors) and that both types of lithium were removed upon charging. Similar structural investigations of a number of possible candidate materials have been undertaken using $^{6/7}$Li NMR spectroscopy, utilizing the ability of the technique to probe local structure and its sensitivity to paramagnetic interactions.[14,107−109]

Of increasing interest, however, is the use of in situ NMR spectroscopy to investigate the production of transient states and the dynamic and chemical processes taking place in real time during the operation of electrochemical devices.[107] In general, in situ experiments are performed (without the use of MAS) on entire devices connected to a potentiostat and NMR spectra are recorded as a function of the charge or discharge state, in approaches pioneered by Tarascon[111] and more recently by Grey.[107,112,113] In a recent example,[113] in situ ^{11}B NMR spectroscopy was used for real-time studies of capacitors to investigate the adsorption of BF_4^- anions on highly porous carbon. Figure 8a shows the experimental setup used, which was modified from a flexible plastic bag cell design, separating the two electrodes so that only one was placed in the NMR coil.[113] This enabled signals from the cathode or anode to be detected separately. Three resonances were observed in the NMR spectrum (see Figure 8b), corresponding to BF_4^- anions strongly bound in the double layers near the carbon electrode, weakly bound ions (at downfield shifts), and a narrow peak resulting from free electrolyte. When the cell was charged, the peaks from strongly and weakly bound BF_4^- began to merge, while at more negative voltages the peak attributed to the strongly bound anions was lost completely. Integration of the ^{11}B NMR resonances (Figure 8c) revealed a gradual decrease in the total signal intensity with decreasing voltage, consistent with the diffusion of BF_4^- ions to the electrode outside of the NMR coil. Similar experiments have been carried out for batteries, supercapacitors, and fuel cells.[107−109]

In addition to battery and capacitor materials, the increasing application of oxide ion conductors in solid oxide fuel cells, sensors, and separators has resulted in considerable NMR investigation of these materials.[109] Despite the need for isotopic enrichment in many cases, ^{17}O NMR spectroscopy has emerged as the method of choice to investigate the local structure and the dynamic processes that take place. An elegant example of this type of study is the work of Kim and Stebbins,[114] where

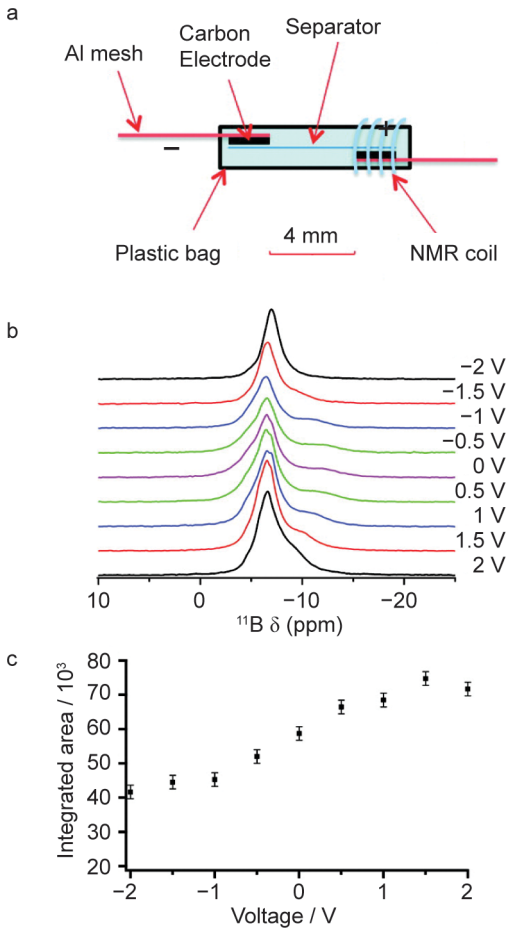

Figure 8. (a) Schematic diagram of a modified supercapacitor cell used for in situ NMR analysis. (b) Stacked plot of ^{11}B NMR spectra obtained while charging the modified supercapacitor between +2 and −2 V. (c) Integrated ^{11}B intensities from (b) plotted as a function of voltage, showing the loss of strongly bound BF_4^- species as the voltage becomes more negative. Adapted from ref 113. Copyright 2011 American Chemical Society.

^{17}O NMR spectroscopy was used to study motion in Y-doped CeO_2, a promising solid oxide electrolyte material. A number of ^{17}O resonances were resolved and could be assigned to environments with differing numbers of Y NNNs. Variable-temperature measurements showed coalescence of some of the peaks, with exchange between sites with Y neighbors occurring at a lower temperature than exchange involving sites distant from the dopant cation. Rapid exchange of all oxygen sites was observed above 400 °C. Such studies will be vital in understanding and designing materials for future applications.

Quadrupolar NMR Spectroscopy of Microporous Materials. Microporous materials have found applications in gas storage and separation, catalysis, and drug delivery, as their structures contain pores and channels of similar size to small molecules. Common microporous frameworks include (alumino)silicate zeolites, phosphate-based frameworks (also typically containing cations of Al, Ga, Si, Mg, etc.), and MOFs (with metal cations connected by organic linker molecules).[115] The basic constituents of these frameworks all contain NMR-active nuclei (many of which are quadrupolar), and in addition, mineralizers and structure-directing agents (SDAs) also contain many nuclei suitable for study. More detailed discussion is also provided in refs 3, 5, 9, 14, and 116.

dx.doi.org/10.1021/ja504734p | J. Am. Chem. Soc. 2014, 136, 15440−15456

While the framework topology of microporous materials can often be determined using diffraction, NMR spectroscopy can provide additional detailed and element-specific information on framework substitution, the nature, disorder, and dynamics of guests within the pores, and the position or disorder of charge-balancing species. NMR crystallography approaches have found particular application in this area,[116,117] as evidenced by recent work on STA-2 (Figure 6), AlPO cloverite, and AlPO-CJ2.[92,118,119] In the latter case, a variety of multinuclear NMR experiments were required in order to quantify the number and type of Al/P environments and understand the framework structure and connectivity. However, by means of two-dimensional correlation experiments, such as the $^{19}F-^{27}Al$ J-HMQC spectrum shown in Figure 9a,[119] information about

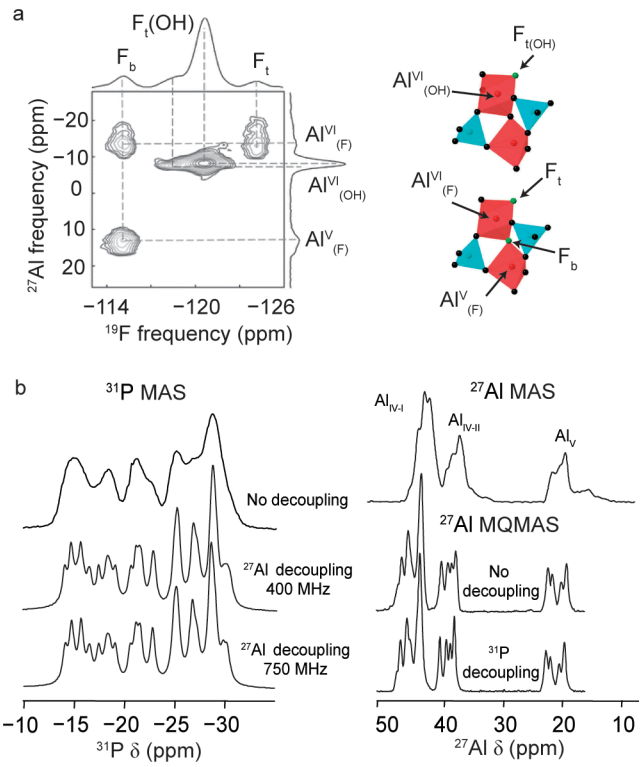

Figure 9. (a) $^{19}F-^{27}Al$ (11.7 T, 15 kHz) J-HMQC spectrum of AlPO-CJ2, enabling the determination of the OH^-/F^- distribution in this framework material. Adapted from ref 119 with permission from the PCCP Owner Societies. (b) ^{31}P (9.4/17.6 T, 14 kHz) and ^{27}Al (17.6 T, 14 kHz) MAS and MQMAS spectra of AlPO-40. Adapted with permission from ref 121. Copyright 2009 John Wiley & Sons, Ltd.

the OH^-/F^- distribution (not easily available from diffraction) was obtained. This spectrum shows that the bridging F^- species (−115 ppm) is connected to both five- and six-fold Al species, while the terminal F^- (−125 ppm) is linked only to six-fold Al. The F^- species (−121 and −118 ppm) are linked to five-fold Al coordinated by OH. In other work, Beitone et al.[120] used a combination of X-ray diffraction and NMR spectroscopy to distinguish between two proposed space groups, $I\bar{4}3m$ and $P\bar{4}3n$, for a new zinc-aluminum phosphate framework, $Zn_3Al_6(PO_4)_{12}\cdot4(tren)\cdot17H_2O$ (MIL-74). More recently, Massiot and co-workers used a range of experiments (including three-dimensional $^{27}Al/^{31}P$ NMR experiments) to demonstrate that the unit cell of AlPO-40 contains 32 Al sites and 32 P sites and is at least 4 times the size proposed initially.[121] The excellent resolution achieved (using decoupling) in the ^{31}P MAS and ^{27}Al MQMAS spectra is shown in Figure 9b.

The great utility of microporous materials is their ability to selectively absorb and interact with guest molecules, either through interactions with framework metals or by adsorption into pores. As oxygen lines the pores of many microporous materials, it might seem that ^{17}O NMR spectroscopy should be a popular choice. However, its application is limited by the low natural abundance of this isotope (0.037%). Many zeolites have been isotopically enriched using postsynthetic exchange with $^{17}O_2$ gas, and although this approach is extremely useful, care must be taken when interpreting peak intensities unless the kinetics and uniformity of the exchange process are understood.[14,19] For aluminosilicates, the resolution of ^{17}O NMR spectra can be limited unless the Si/Al ratio is high, but for materials with little cation disorder, oxygen species can be resolved using MQMAS or DOR. As shown by the impressive work on the zeolite ferrierite, where 10 oxygen species are distinguished, variable-field measurements are often vital.[122] Enrichment of phosphate frameworks is considerably more challenging, as the SDA and the framework itself can break down at the temperatures used for gas exchange. Although solvothermal synthesis using liquid $H_2{}^{17}O$ is possible, this is costly and cost-inefficient, as relatively little of the enriched material ends up in the framework. It has recently been shown, however, that cost-efficient ^{17}O enrichment is possible using ionothermal synthesis, where an ionic liquid is used as a solvent and only a small amount (10−20 μL) of $H_2{}^{17}O(l)$ is added.[123] Cost-effective ^{17}O enrichment of MOFs (including MIL-53(Al) and CPO-27-Mg) has also been recently demonstrated in the work by He et al.,[124] in which the reactants were mixed and sealed in an autoclave that contained a small amount of $H_2{}^{17}O(l)$. This work was also able to distinguish between bridging oxide and hydroxide ligands in UiO-66, a task that would be almost impossible to achieve by diffraction techniques.[124]

MOFs exhibit greater structural variation than zeolites or phosphate-based frameworks because of the larger number of possible combinations of organic linkers and metals. Furthermore, with the growing possibility of postsynthetic modifications, even greater variation of the structure is possible.[115] The study of MOFs using NMR spectroscopy has generally been limited to ^1H and ^{13}C ($I = {}^1/_2$) experiments, although there have been some recent investigations of the metals.[9,116] For example, ^{27}Al and ^{45}Sc NMR spectroscopy has been used to study the motion and flexibility in MIL-53, where it is known that the MOF exhibits a so-called breathing motion, increasing the unit cell volume by up to 230% when a guest molecule is adsorbed.[125,126] In addition, ^2H NMR spectroscopy has been recently used to study the dynamics of the linker molecules in a number of MOFs, revealing motions such as C_2 rotation of the benzene rings in terephthalate-based MOFs.[127,128]

Quadrupolar NMR Spectroscopy in the Earth Sciences. Solid-state NMR spectroscopy has had a significant impact in the field of geochemistry, as ^{29}Si ($I = {}^1/_2$) NMR spectroscopy has been used extensively to study minerals, glasses, and clays. However, the main constituents of our planet, crustal aluminosilicates and deep-earth magnesium silicates, also contain quadrupolar nuclei, primarily ^{17}O, ^{27}Al, and ^{25}Mg.[8,10,14] Natural minerals are complex multicomponent systems that display considerable disorder, arising from the variation of cation/anion site occupancies or the detailed local

dx.doi.org/10.1021/ja504734p | J. Am. Chem. Soc. 2014, 136, 15440−15456

structure and bonding. X-ray diffraction provides information on the average structure, and it falls to spectroscopy to probe the local environment and dynamic processes in more detail. As shown in Table 1, ^{27}Al offers perhaps the best prospects for straightforward study, with 100% natural abundance and high γ. For ^{17}O, isotopic enrichment is often required, while the relatively low natural abundance, low γ, and large quadrupolar broadening combine to make ^{25}Mg NMR spectroscopy more of a challenge.

Many minerals and clays have been studied using ^{27}Al NMR spectroscopy,[8,10,14] although quadrupolar broadening prevents the resolution of distinct species unless MQMAS is used. The NMR parameters can often be related to local structural features such as the distortion of coordination polyhedra or variation in cation−oxygen bond distances.[2,8,10] The dependence of the ^{27}Al chemical shift on the coordination number has been exploited to help determine substitution mechanisms in natural minerals.[2,8,10] It is difficult to determine the effect of NNN substitutions (e.g., cation site disorder) in aluminosilicates because of the quadrupolar broadening. More recently, however, the combination of experiment and calculation has offered an improved approach. This was elegantly demonstrated in the recent study by Massiot and co-workers, who investigated Al/Si ordering in gehlenite, $Ca_2Al_2SiO_7$.[91] By means of MAS, MQMAS, and two-dimensional ^{29}Si/^{27}Al HMQC experiments, seven distinct Al sites, $Al(OAl)_{4-p}(OSi)_p$ and $Al(OAl)_{3-p}(OSi)_p$ were identified. Comparison to the results of DFT calculations on model structures determined that a purely random distribution of Al and Si (i.e., not respecting Lowenstein's rule[129]) was present. This work really shows what is possible when state-of-the-art experiments and calculations are combined and reflects the future direction of NMR crystallography.

Dynamic processes are of considerable interest in the Earth sciences, and many examples of investigations using quadrupolar NMR spectroscopy (e.g., ^{2}H, ^{17}O, ^{27}Al, and ^{25}Mg) are known.[8,10,14] Of particular interest is the differentiation between static and dynamic disorder, as, for example, in the case of the humite minerals shown in Figure 7 and described in detail above. In general, an understanding of OH^-/F^- disorder in natural minerals is a challenge, and it is particularly difficult to probe using diffraction. Exchange between different sites in minerals can be probed using variable-temperature experiments, with notable examples including exchange of six- and eight-coordinate Na environments in nepheline, $Na_{0.95}K_{0.05}AlSiO_4$, using ^{23}Na NMR spectroscopy[14,130] and exchange of the two Mg sites in forsterite, α-Mg_2SiO_4, using ^{25}Mg NMR spectroscopy.[14,131]

The study of deep-earth silicate minerals is hampered by the requirement to synthesize these materials at high pressure (e.g., up to 130 GPa).[8,132] The use of a piston cylinder or a multianvil apparatus can restrict the amount of material available (to just a few milligrams in the latter case), limiting the sensitivity and increasing the technical challenge of the measurements. Nonetheless, the recent advances in probe technology and greater availability of high magnetic fields have facilitated the study of such systems. Over the last few decades it has been recognized that the nominally anhydrous minerals in the mantle can store significant quantities of hydrogen, typically termed "water", at defects in the crystal lattice.[8] The advantages of using NMR spectroscopy to study these materials were highlighted in recent work combining experiment and DFT calculations to investigate the hydration of wadsleyite, β-Mg_2SiO_4.[133] Significant differences were seen in the STMAS (20.0 T) spectra of anhydrous and hydrous wadsleyite, as shown in Figure 10a,b, with a decrease in the intensity of O1

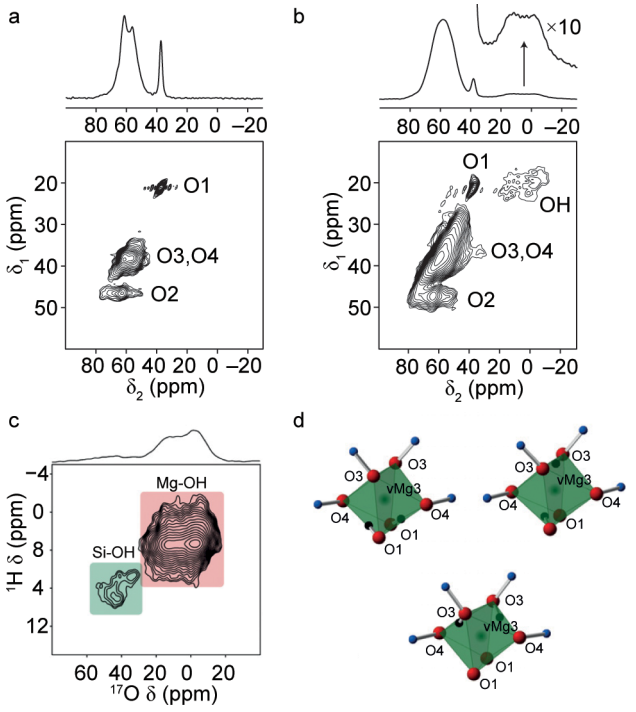

Figure 10. (a, b) ^{17}O (20.0 T, 30 kHz) STMAS NMR spectra of (a) anhydrous and (b) hydrous (3 wt %) wadsleyite, β-Mg_2SiO_4, showing a decrease in the intensity of the resonance attributed to O1 and a corresponding increase in a broader resonance thought to be associated with hydroxyl oxygens. (c) ^{1}H/^{17}O (20.0 T, 30 kHz) CP HETCOR spectrum of hydrous wadsleyite, showing two different types of hydroxyl species. (d) Possible structural models for the defect sites in hydrous wadsleyite determined using DFT calculations. Adapted from ref 133 with permission from The Royal Society of Chemistry.

and an increase in a broad resonance attributed to OH^-. DFT calculations showed that a Mg3 vacancy compensates for the substitution and that the ^{1}H spectrum could only be matched by protonation of not just O1 but also the O3/O4 silicate oxygens. This was confirmed by ^{1}H/^{17}O correlation experiments, as shown in Figure 10c, where Si−OH and Mg−OH species can be identified.[133]

Silicate glasses are of considerable importance at the Earth's surface, and their study can provide information on the composition of volcanic eruptions, heat and mass transfer within the Earth, and the effects of weathering at the surface.[10,14] Such glasses are also of interest in materials science and technology and in the remediation of nuclear waste. The lack of long-range order in glasses has provoked considerable interest in their study using NMR spectroscopy, an area that could form the topic of a complete review in itself.[134] Generally, the composition, speciation, and cation disorder can be probed, although the variation in local geometry results in a distribution of NMR parameters, and while chemically distinct species can be identified, resolution of individual sites is not possible.[134] In the context of the Earth sciences, ^{27}Al and ^{17}O NMR spectroscopy are perhaps the most useful approaches, with ^{27}Al NMR spectra providing information on the Al coordination number, while ^{17}O

dx.doi.org/10.1021/ja504734p | J. Am. Chem. Soc. 2014, 136, 15440−15456

MQMAS experiments are able to resolve Si−O−Si, Si−O−Al, and Al−O−Al species, thus probing the extent of framework disorder.[135−137] Experiments on samples that have been rapidly quenched from high temperature or experiments carried out under higher pressures can be used to quantify the structural changes observed in glasses, with the most notable changes being increased coordination of Al and Si species with increasing pressure.[10,14,134]

Quadrupolar NMR Spectroscopy of Organic and Biological Materials. As one might expect, the most commonly studied nuclei in NMR studies of organic and biological materials are ^{1}H, ^{13}C, and ^{15}N.[2,6,7] As all have $I = {}^{1}/_{2}$, high-resolution spectra are relatively easy to acquire (if fast MAS or high-power decoupling is available) and the sensitivity can be enhanced by using CP. However, quadrupolar nuclei, such as ^{23}Na, ^{25}Mg, ^{39}K, ^{43}Ca, ^{63}Cu, and ^{67}Zn, are abundant in biological systems, including proteins, enzymes, and cell nuclei,[14,138,139] while nuclei such as ^{23}Na, ^{7}Li, and ^{133}Cs have pharmacological applications. In addition to the challenges faced for inorganic solids, there are often relatively few metal sites in biological systems, and many of the relevant species have low receptivities and/or significant quadrupolar broadening. This emerging area, therefore, had been facilitated more than most by the use of higher magnetic fields, advances in hardware, and the introduction of sensitivity enhancement schemes.[14,33]

It has been estimated that at least one-third of all proteins and enzymes that have been purified require metals for their biological function.[14] One such example is zinc-containing proteins, where the metal center plays an important role in structure and catalysis. There have been relatively few solid-state ^{67}Zn NMR studies because of the low natural abundance (4.1%), low receptivity, and large quadrupole moment of ^{67}Zn (as shown in Figure 4). Despite these challenges, in impressive work Lipton et al.[140] were able to obtain ^{67}Zn CPMG NMR spectra for the wild type (WT) and the H265A mutant of *Aquifex aeolicus* LpxC. A difference was observed in the ^{67}Zn spectrum with pH, as shown in Figure 11 for the WT protein. The appearance of a third Zn species at high pH (with C_Q = 14.3 MHz) was attributed to changes in the protonation state of a nearby histidine residue by comparison of the experimental measurements to theoretical calculations, providing insight into the structure of the protein under physiological conditions.

As with protein studies, investigations of biomaterials using NMR spectroscopy have also primarily exploited spin $I = {}^{1}/_{2}$ nuclei such as ^{13}C, ^{15}N, and ^{31}P because of the ease of spectral acquisition. However, of considerable potential is ^{43}Ca ($I = {}^{7}/_{2}$) NMR spectroscopy, as calcium can be found in naturally occurring bone, tooth enamel, and dentin.[141] Calcium can be challenging to study because of its very low natural abundance (0.135%) and the high cost of isotopic enrichment. A number of ^{43}Ca NMR investigations of bone and bone-related minerals have been performed,[141] with the first spectra of natural biominerals, a horse bone and a cow tooth, appearing in 2010.[142] In this work, a combination of ^{43}Ca solid-state NMR and Ca K-edge X-ray absorption spectroscopy provided information about the calcium coordination shell and demonstrated a correlation of the ^{43}Ca chemical shift with the (average) Ca−O bond distance.[142] The complex nature of bone (a composite material in which hydroxyapatite-like phases and an organic matrix are combined) has also led to considerable study of model apatite systems. In addition to the study of pure hydroxyapatite, $Ca_{10}(PO_4)_6(OH)_2$, which

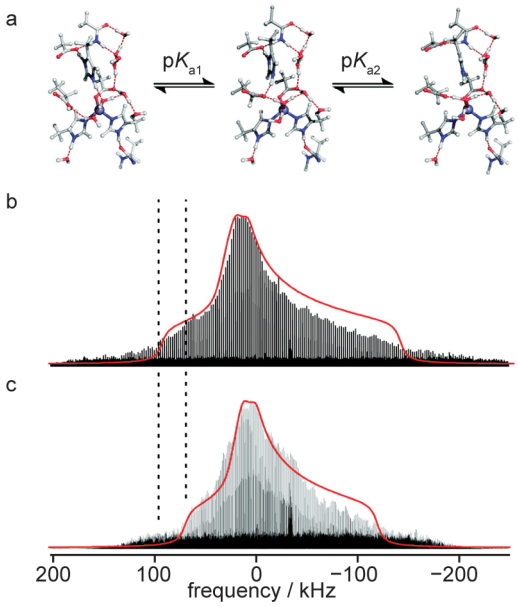

Figure 11. (a) Changes in the structure of the zinc-containing protein *Aquifex aeolicus* LpxC with pH variation, showing deprotonation of initially a glutamine residue and subsequently a histidine residue. (b, c) ^{67}Zn (18.8 T) CPMG spectra of a static sample of wild-type LpxC at (b) pH 8.7 and (c) pH 6. The simulated line shapes (shown in red) highlight the change in C_Q observed. Adapted from ref 140. Copyright 2008 American Chemical Society.

contains two distinct Ca sites, investigations have also focused on possible substitutions of CO_3^{2-}, HPO_4^{2-}, Na^+, and Mg^{2+} into the apatite lattice.[142] The importance of biomaterials in the modern world will ensure that this is an area of active research, with great benefit being obtained from higher magnetic fields.

Nitrogen is a key component of many biological, organic, and pharmacological materials. The most abundant isotope, ^{14}N (natural abundance 99.6%), is quadrupolar (I = 1), although earlier studies focused on ^{15}N ($I = {}^{1}/_{2}$) despite its low natural abundance (0.36%). As described above, ^{14}N does not exhibit a CT, and observation of all species (except those with symmetrical environments) was prohibitively time-consuming until recent years. An increase in the availability of high-field measurements (and concomitant increases in sensitivity) brought some progress for wideline measurements, but perhaps the most significant advance in recent years has been the use of indirect detection experiments.[14,85−87] These MAS-based methods exploit the transfer of magnetization between a spin $I = {}^{1}/_{2}$ nucleus (typically ^{1}H or ^{13}C) and ^{14}N, with the ^{14}N MAS spectrum exhibiting line shapes broadened by the second- and sometimes third-order quadrupolar interaction. These have been used to provide information on ^{14}N quadrupolar couplings, C−N internuclear distances, and dynamics in amino acids, small peptides, and pharmaceutical compounds,[14,85−87] representing an exciting area for future applications.

8. CHALLENGES AND OUTLOOK

Since the first discussion of quadrupolar interactions in 1950[143] paved the way for the study of nuclei with spin $I > {}^{1}/_{2}$ by NMR spectroscopy, the impressive developments in sophisticated hardware and the complex yet elegant pulse sequences introduced have enabled a wide application across the scientific disciplines. Despite often being viewed as the poor relation of I

= $^1/_2$ NMR spectroscopy, the study of quadrupolar nuclei, although admittedly technically more challenging, has the potential to offer more information (as a result of the additional interactions the nuclear spins experience) and is applicable to a greater proportion of the periodic table. An ongoing challenge is unquestionably the acquisition of high-resolution spectra (or alternatively the separation of the components of a composite spectral line shape) in a cost-efficient and rapid manner. The presence of second-order quadrupolar broadening limits the utility of MAS, but we can surely look forward in the future to advances in technology and hardware that will significantly ease the practical implementation (and thus improve the performance) of experiments such as DOR[42] and STMAS.[48] It is indisputable that NMR study of quadrupolar nuclei was revolutionized by the introduction of MQMAS,[44] and this has enabled a far greater applicability than was envisaged in the early 1990s. However, difficulties with this method still remain, including the need for improved sensitivity both in absolute terms and per unit time. Possible solutions could be the use of more complex pulses or changes to the way spectra are acquired. It has been demonstrated that some multidimensional spectra can be obtained in a single scan or step,[144] and while this is currently difficult to implement in every experiment, future software advances may make this routine for many spectra in the near future.

Although the higher MAS rates currently available contribute to improved spectral resolution, the limited sample volumes compound the second significant challenge that afflicts NMR spectroscopy of quadrupolar nuclei, namely, sensitivity. The increasing availability of high-field measurements will certainly help ameliorate this problem, and the recent developments in microcoil technology (enabling extremely strong rf fields to be achieved) should mitigate, at least to some extent, the limiting sensitivity of small volumes.[145] This will also enable better decoupling to be used, therefore, simultaneously aiding resolution. It may be that additional advances will also be forthcoming if increased effort can be expended on the development of better methods for isotopic enrichment, as modifications to existing synthetic procedures may be able to significantly reduce the cost in terms of both time and money. However, perhaps the technique generating the most interest in this regard is dynamic nuclear polarization (DNP),[146] in which the transfer of polarization from unpaired electrons to nuclei is able to provide significant signal enhancements. Although to date this technique has largely been applied to organic solids, porous materials, and surfaces, exploiting both rapid spin diffusion among ^{1}H spins (prior to transfer to the nuclear species of interest) and easier introduction of the polarizing agent, more recent work has been focused on quadrupolar nuclei and inorganic solids.[147−149] In view of the need for the development of reliable protocols for sample preparation and an improved understanding of the experiment-, sample-, and distance-dependent enhancements observed, only time will tell whether DNP will prove to be the panacea that has been suggested, but it is certainly an exciting area requiring future research investment.

One clear future direction for improving the understanding of solid-state structure is the need for a closer relationship between the complementary diffraction-based and spectroscopic methods. This will enable the construction of a detailed picture of a material on a range of length and time scales, which is essential if its physical and chemical properties are to be understood and therefore exploited. Computation may well be the key here, not only easing the understanding, interpretation, and assignment of the complex spectral line shapes observed but also enabling the prediction of NMR parameters for potential structural models and subsequent comparison to NMR experimental measurements. The greatest impact might well arise from the widening interest in methods for the generation of possible structural models prior to the calculation of NMR parameters, both in terms of high-throughput calculations in disordered systems and from first principles (as in the ab initio random structure searching (AIRSS) approach[150]).

An important goal for NMR spectroscopy is understanding the structural changes that occur during phase transitions, adsorption, and chemical reactions. While progress has been made in many areas using ex situ measurements (i.e., following an external reaction or process by quenching at various stages and subsequently analyzing the material produced), the ultimate aim would be to follow these process in situ, with the procedure carried out inside the spectrometer directly. Variable-temperature experiments are possible, although measurements under more extreme conditions remain technically challenging and often the realm of specialists. Measurements have been made in situ and in operando,[107,151,152] but the need to consider problems such as the flow of reactants and removal of products in a reaction, changes in electrochemical properties, density, or volume of a solid during a phase transition, and the generation of gases in a reaction, make the combination of these experiments with sample rotation extremely challenging. However, the potential impact of such measurements does make this an essential direction for future research.

It is clear that much more technological and methodological development is required before NMR spectroscopy of quadrupolar nuclei can achieve anywhere near its full potential. However, the consistent progress made over the last few decades augurs well for further advances in the years to come. It is to be hoped that researchers of the future will view NMR spectroscopy as an important component of a suite of analytical techniques that should be combined to provide detailed information on structure, disorder, and dynamics in the solid state.

AUTHOR INFORMATION

Corresponding Author

sema@st-andrews.ac.uk

Notes

The authors declare no competing financial interest.

ACKNOWLEDGMENTS

The authors acknowledge the EPSRC for the award of a studentship to S.S. The authors also thank Dr. Daniel Dawson and Dr. Valerie Seymour for their help in the preparation of this article.

REFERENCES

(1) Apperley, D. C.; Harris, R. K.; Hodgkinson, P. *Solid State NMR: Basic Principles and Practice*; Momentum Press: New York, 2012.
(2) MacKenzie, K. J. D.; Smith, M. E. *Multinuclear Solid-State NMR of Inorganic Materials*; Pergamon Press: Oxford, U.K., 2002.
(3) Klinowski, J. *Prog. Nucl. Magn. Reson. Spectrosc.* **1984**, *16*, 237−309.
(4) Eckert, H. *Prog. Nucl. Magn. Reson. Spectrosc.* **1992**, *24*, 159−293.
(5) Klinowski, J. *Anal. Chim. Acta* **1993**, *283*, 929−965.

(6) Brown, S. P. *Macromol. Rapid Commun.* **2009**, *30*, 688−716.
(7) Hodgkinson, P. *Annu. Rep. NMR Spectrosc.* **2010**, *72*, 185−223.
(8) Ashbrook, S. E.; Griffin, J. M. *Annu. Rep. NMR Spectrosc.* **2013**, *79*, 241−332.
(9) Sutrisno, A.; Huang, Y. *Solid State Nucl. Magn. Reson.* **2013**, *49*−*50*, 1−11.
(10) Stebbins, J. F.; Xue, X. Y. *Spectroscopic Methods in Mineralogy and Materials Sciences*; Mineralogical Society of America: Chantilly, VA, 2014.
(11) Andrew, E. R.; Bradbury, A.; Eades, R. G. *Nature* **1958**, *182*, 1659.
(12) Hodgkinson, P. *Prog. Nucl. Magn. Reson. Spectrosc.* **2005**, *46*, 197−222.
(13) Vega, A. J. *eMagRes* **2010**, DOI: 10.1002/9780470034590.emrstm0431.pub2.
(14) *NMR of Quadrupolar Nuclei in Solid Materials*; Wasylishen, R. E., Ashbrook, S. E., Wimperis, S., Eds.; John Wiley & Sons: Chichester, U.K., 2012.
(15) Fernandez, C.; Pruski, M. *Top. Curr. Chem.* **2012**, *306*, 119−188.
(16) Freitas, J. C. C.; Smith, M. E. *Annu. Rep. NMR Spectrosc.* **2012**, *75*, 25−114.
(17) Bräuniger, T.; Jansen, M. *Z. Anorg. Allg. Chem.* **2013**, *639*, 857−879.
(18) Chapman, R. P.; Widdifield, C. M.; Bryce, D. L. *Prog. Nucl. Magn. Reson. Spectrosc.* **2009**, *55*, 215−237.
(19) Ashbrook, S. E.; Smith, M. E. *Chem. Soc. Rev.* **2006**, *35*, 718−735.
(20) Ashbrook, S. E.; Duer, M. J. *Concepts Magn. Reson.* **2006**, *28A*, 183−248.
(21) Ashbrook, S. E.; Antonijevic, S.; Berry, A. J.; Wimperis, S. *Chem. Phys. Lett.* **2002**, *364*, 634−642.
(22) Amri, M.; Ashbrook, S. E.; Dawson, D. M.; Griffin, J. M.; Walton, R. I.; Wimperis, S. *J. Phys. Chem. C* **2012**, *116*, 15048−15057.
(23) Engelhardt, G.; Kentgens, A. P. M.; Koller, H.; Samoson, A. *Solid State Nucl. Magn. Reson.* **1999**, *15*, 171−180.
(24) Schurko, R. W. *eMagRes* **2011**, DOI: 10.1002/9780470034590.emrstm1199.
(25) O'Dell, L. A.; Schurko, R. W. *Chem. Phys. Lett.* **2008**, *464*, 97−102.
(26) O'Dell, L. A.; Rossini, A. J.; Schurko, R. W. *Chem. Phys. Lett.* **2009**, *468*, 330−335.
(27) Schurko, R. W. *Acc. Chem. Res.* **2013**, *46*, 1985−1995.
(28) O'Dell, L. A. *Solid State Nucl. Magn. Reson.* **2013**, *55*−*56*, 28−41.
(29) Meiboom, S.; Gill, D. *Rev. Sci. Instrum.* **1958**, *29*, 688−691.
(30) Madhu, P. K.; Goldbourt, A.; Frydman, L.; Vega, S. *Chem. Phys. Lett.* **1999**, *307*, 41−47.
(31) Kentgens, A. P. M.; Verhagen, R. *Chem. Phys. Lett.* **1999**, *300*, 435−443.
(32) Seigel, R.; Nakashima, T. K.; Wasylishen, R. E. *Chem. Phys. Lett.* **2004**, *388*, 441−445.
(33) Nakashima, T. T.; Wasylishen, R. E. *eMagRes* **2011**, DOI: 10.1002/9780470034590.emrstm1200.
(34) Perras, F. A.; Viger-Gravel, J.; Burgess, K. M. N.; Bryce, D. L. *Solid State Nucl. Magn. Reson.* **2013**, *51*−*52*, 1−15.
(35) Johnston, K. E.; O'Keefe, C. A.; Gauvin, R. M.; Trébosc, J.; Delevoye, L.; Amoureux, J. P.; Popoff, N.; Taoufik, M.; Oudatchin, K.; Schurko, R. W. *Chem.—Eur. J.* **2013**, *19*, 12396−12414.
(36) Griffin, J. M.; Berry, A. J.; Ashbrook, S. E. *Solid State Nucl. Magn. Reson.* **2011**, *40*, 91−99.
(37) Burgess, K. M. N.; Xu, Y.; Leclerc, M. C.; Bryce, D. L. *Inorg. Chem.* **2014**, *53*, 552−561.
(38) Hamaed, H.; Johnston, K. E.; Cooper, B. F. T.; Terskikh, V. V.; Ye, E.; Macdonald, C. L. B.; Arnold, D. C.; Schurko, R. W. *Chem. Sci.* **2014**, *5*, 982−995.
(39) Hamaed, H.; Ye, E.; Udachin, K.; Schurko, R. W. *J. Phys. Chem. B* **2010**, *114*, 6014−6022.
(40) O'Dell, L. A.; Schurko, R. W. *J. Am. Chem. Soc.* **2009**, *131*, 6658−6659.
(41) Attrell, R. J.; Widdifield, C. M.; Korobkov, I.; Bryce, D. L. *Cryst. Growth Des.* **2012**, *12*, 1641−1653.
(42) Samoson, A.; Lippmaa, E.; Pines, A. *Mol. Phys.* **1988**, *65*, 1013−1018.
(43) Mueller, K. T.; Sun, B. Q.; Chingas, G. C.; Zwanziger, J. W.; Terao, T.; Pines, A. *J. Magn. Reson.* **1990**, *86*, 470−487.
(44) Frydman, L.; Harwood, J. S. *J. Am. Chem. Soc.* **1995**, *117*, 5367−5368.
(45) Goldbourt, A.; Madhu, P. K. *Annu. Rep. NMR Spectrosc.* **2004**, *54*, 81−153.
(46) Rocha, J.; Morais, C. M.; Fernandez, C. *Top. Curr. Chem.* **2005**, *246*, 141−194.
(47) Gan, Z. *J. Am. Chem. Soc.* **2000**, *122*, 3242−3243.
(48) Ashbrook, S. E.; Wimperis, S. *Prog. Nucl. Magn. Reson. Spectrosc.* **2004**, *45*, 53−108.
(49) Gan, Z.; Kwak, H. T. *J. Magn. Reson.* **2004**, *168*, 346−351.
(50) Colaux, H.; Dawson, D. M.; Ashbrook, S. E. *J. Phys. Chem. A* **2014**, *118*, 6018−6025.
(51) Perras, F. A.; Bryce, D. L. *J. Magn. Reson.* **2011**, *213*, 82−89.
(52) Perras, F. A.; Bryce, D. L. *J. Chem. Phys.* **2013**, *138*, No. 174202.
(53) Perras, F. A.; Bryce, D. L. *J. Magn. Reson.* **2014**, *242*, 23−32.
(54) Ashbrook, S. E.; McManus, J.; Thrippleton, M. J.; Wimperis, S. *Prog. Nucl. Magn. Reson. Spectrosc.* **2009**, *55*, 160−181.
(55) Sternheimer, R. *Phys. Rev.* **1954**, *95*, 736−750.
(56) O'Dell, L. *Prog. Nucl. Magn. Reson. Spectrosc.* **2011**, *59*, 295−318.
(57) Hoatson, G. L.; Vold, R. L. *NMR: Basic Princ. Prog.* **1994**, *32*, 1−67.
(58) Colin, J. F.; Bataille, T.; Ashbrook, S. E.; Audebrand, N.; Le Polles, L.; Pivan, J. Y.; Le Fur, E. *Inorg. Chem.* **2006**, *45*, 6034−6040.
(59) Johnston, K. E.; Tang, C. C.; Parker, J. E.; Knight, K. S.; Lightfoot, P.; Ashbrook, S. E. *J. Am. Chem. Soc.* **2010**, *132*, 8732−8746.
(60) Hanna, J. V.; Smith, M. E.; Whitfield, H. J. *J. Am. Chem. Soc.* **1996**, *118*, 5772−5777.
(61) Sheppard, D.; Tugarinov, V. *J. Magn. Reson.* **2010**, *203*, 316−322.
(62) Alemany, L. B.; Steuernagel, S.; Amoureux, J. P.; Callender, R. L.; Barron, A. R. *Solid State Nucl. Magn. Reson.* **1999**, *14*, 1−18.
(63) Pickard, C. J.; Mauri, F. *Phys. Rev. B* **2001**, *63*, No. 245101.
(64) Cuny, J.; Messaoudi, S.; Alonzo, V.; Furet, E.; Halet, J. F.; Le Fur, E.; Ashbrook, S. E.; Pickard, C. J.; Gautier, R.; Le Polles, L. *J. Comput. Chem.* **2008**, *29*, 2279−2287.
(65) Charpentier, T. *Solid State Nucl. Magn. Reson.* **2011**, *40*, 1−20.
(66) Bonhomme, C.; Gervais, C.; Babonneau, F.; Coelho, C.; Pourpoint, F.; Azaïs, T.; Ashbrook, S. E.; Griffin, J. M.; Yates, J. R.; Mauri, F.; Pickard, C. J. *Chem. Rev.* **2012**, *112*, 5733−5779.
(67) Ashbrook, S. E.; Le Polles, L.; Pickard, C. J.; Berry, A. J.; Wimperis, S.; Farnan, I. *Phys. Chem. Chem. Phys.* **2007**, *9*, 1587−1598.
(68) Ashbrook, S. E.; Berry, A. J.; Hibberson, W. O.; Steuernagel, S.; Wimperis, S. *J. Am. Chem. Soc.* **2003**, *125*, 11824−11825.
(69) *NMR Crystallography*; Harris, R. K., Wasylishen, R. E., Duer, M. J., Eds.; John Wiley & Sons: Chichester, U.K., 2009.
(70) Martineau, C.; Cadiau, A.; Bouchevreau, B.; Senker, J.; Taulelle, F.; Adil, K. *Dalton Trans.* **2012**, *41*, 6232−6241.
(71) Amoureux, J. P.; Trébosc, J.; Delevoye, L.; Lafon, O.; Hu, B.; Wang, Q. *Solid State Nucl. Magn. Reson.* **2009**, *35*, 12−18.
(72) Ashbrook, S. E.; Cutajar, M.; Pickard, C. J.; Walton, R. I.; Wimperis, S. *Phys. Chem. Chem. Phys.* **2008**, *10*, 5754−5764.
(73) Wiench, J. W.; Pruski, M. *Solid State Nucl. Magn. Reson.* **2004**, *26*, 51−55.
(74) Montouillout, V.; Morais, C. M.; Douy, A.; Fayon, F.; Massiot, D. *Magn. Reson. Chem.* **2006**, *44*, 770−775.
(75) Iuga, D.; Morais, C.; Gan, Z.; Neuville, D. R.; Cormier, L.; Massiot, D. *J. Am. Chem. Soc.* **2005**, *127*, 11540−11541.
(76) Ashbrook, S. E.; Wimperis, S. *Mol. Phys.* **2000**, *98*, 1−26.
(77) Amoureux, J. P.; Pruski, M. *Mol. Phys.* **2002**, *100*, 1595−1613.
(78) Ashbrook, S. E.; Wimperis, S. *J. Chem. Phys.* **2004**, *120*, 2719−2731.

(79) Ashbrook, S. E.; Wimperis, S. *J. Chem. Phys.* **2009**, *131*, No. 194509.
(80) Lu, X.; Lafon, O.; Trébosc, J.; Tricot, G.; Delevoye, L.; Méar, F.; Montagne, L.; Amoureux, J. P. *J. Chem. Phys.* **2012**, *137*, No. 144201.
(81) Hu, B.; Trébosc, J.; Amoureux, J. P. *J. Magn. Reson.* **2008**, *192*, 112−122.
(82) Levitt, M. H. *J. Chem. Phys.* **2008**, *128*, No. 052205.
(83) Mali, G.; Fink, G.; Taulelle, F. *J. Chem. Phys.* **2004**, *120*, 2835−2845.
(84) Eden, M.; Zhou, D.; Yu, J. *Chem. Phys. Lett.* **2006**, *431*, 397−403.
(85) Gan, Z. *J. Am. Chem. Soc.* **2006**, *128*, 6040−6041.
(86) Cavadini, S.; Antonijevic, A.; Lupulescu, A.; Bodenhausen, G. *J. Magn. Reson.* **2006**, *182*, 168−172.
(87) Cavadini, S. *Prog. Nucl. Magn. Reson. Spectrosc.* **2010**, *56*, 46−77.
(88) de Lacaillerie, J. B. D.; Fretigny, C.; Massiot, D. *J. Magn. Reson.* **2008**, *192*, 244−251.
(89) Ferrara, C.; Tealdi, C.; Pedone, A.; Menziani, M. C.; Rossini, A. J.; Pintacuda, G.; Mustarelli, P. *J. Phys. Chem. C* **2013**, *117*, 23451−23458.
(90) Johnston, K. E.; Mitchell, M. R.; Blanc, F.; Lightfoot, P.; Ashbrook, S. E. *J. Phys. Chem. C* **2013**, *117*, 2252−2265.
(91) Florian, P.; Veron, E.; Green, T. F. G.; Yates, J. R.; Massiot, D. *Chem. Mater.* **2012**, *24*, 4068−4079.
(92) Seymour, V. R.; Eschenroeder, E. C. V.; Castro, M.; Wright, P. A.; Ashbrook, S. E. *CrystEngComm* **2013**, *15*, 8668−8679.
(93) Blanc, F.; Middlemiss, D. S.; Gan, Z.; Grey, C. P. *J. Am. Chem. Soc.* **2011**, *133*, 17662−17672.
(94) Ashbrook, S. E.; Dawson, D. M. *Acc. Chem. Res.* **2013**, *46*, 1964−1974.
(95) Florian, P.; Massiot, D. *CrystEngComm* **2013**, *15*, 8623−8626.
(96) O'Dell, L. A.; Ratcliffe, C. I. *eMagRes* **2011**, DOI: 10.1002/9780470034590.emrstm1209.
(97) Vold, R. L.; Hoatson, G. L. *J. Magn. Reson.* **2009**, *198*, 57−72.
(98) Cutajar, M.; Ashbrook, S. E.; Wimperis, S. *Chem. Phys. Lett.* **2006**, *423*, 276−281.
(99) Thrippleton, M. J.; Cutajar, M.; Wimperis, S. *Chem. Phys. Lett.* **2008**, *452*, 233−238.
(100) Hampson, M. R.; Hodgkinson, P.; Evans, J. S. O.; Harris, R. K.; King, I. J.; Allen, S.; Fayon, F. *Chem. Commun.* **2004**, 392−393.
(101) Antonijevic, S.; Ashbrook, S. E.; Biedasek, S.; Walton, R. I.; Wimperis, S.; Yang, H. *J. Am. Chem. Soc.* **2006**, *128*, 8054−8062.
(102) Ashbrook, S. E.; Berry, A. J.; Wimperis, S. *J. Am. Chem. Soc.* **2001**, *123*, 6360−6366.
(103) Griffin, J. M.; Wimperis, S.; Berry, A. J.; Pickard, C. J.; Ashbrook, S. E. *J. Phys. Chem. C* **2009**, *113*, 465−471.
(104) Griffin, J. M.; Miller, A. J.; Berry, A. J.; Wimperis, S.; Ashbrook, S. E. *Phys. Chem. Chem. Phys.* **2010**, *12*, 2989−2998.
(105) Griffin, J. M.; Yates, J. R.; Berry, A. J.; Wimperis, S.; Ashbrook, S. E. *J. Am. Chem. Soc.* **2010**, *132*, 15651−15660.
(106) Ashbrook, S. E.; Cutajar, M.; Griffin, J. M.; Lethbridge, Z. A.; Walton, R. I.; Wimperis, S. *J. Phys. Chem. C* **2009**, *113*, 10780−10789.
(107) Blanc, F.; Leskes, M.; Grey, C. P. *Acc. Chem. Res.* **2013**, *46*, 1952−1963.
(108) Grey, C. P.; Dupre, N. *Chem. Rev.* **2004**, *104*, 4493−4512.
(109) Blanc, F.; Spencer, L.; Goward, G. R. *eMagRes* **2011**, DOI: 10.1002/9780470034590.emrstm1215.
(110) Yoon, W. S.; Grey, C. P.; Balasubramanian, M.; Yang, X. Q.; Fischer, D. A.; McBreen, J. *Electrochem. Solid-State Lett.* **2004**, *7*, A53−A55.
(111) Letellier, M.; Chevallier, F.; Clinard, C.; Frackowiak, E.; Rouzaud, J. N.; Beguin, F.; Morcrette, M.; Tarascon, J. M. *J. Chem. Phys.* **2003**, *118*, 6038−6045.
(112) Key, B.; Bhattacharyya, R.; Morcrette, M.; Seznec, V.; Tarascon, J. M.; Grey, C. P. *J. Am. Chem. Soc.* **2009**, *131*, 9239−9249.
(113) Wang, H.; Köster, T. K. J.; Trease, N. M.; Ségalini, J.; Taberna, P. L.; Simon, P.; Gogotsi, Y.; Grey, C. P. *J. Am. Chem. Soc.* **2011**, *133*, 19270−19273.
(114) Kim, N.; Stebbins, J. F. *Chem. Mater.* **2007**, *19*, 5742−5747.
(115) Wright, P. A. *Microporous Framework Solids*, 1st ed.; The Royal Society of Chemistry: Cambridge, U.K., 2008.
(116) Ashbrook, S. E.; Dawson, D. M.; Seymour, V. R. *Phys. Chem. Chem. Phys.* **2014**, *16*, 8223−8242.
(117) Taulelle, F.; Bouchevreau, B.; Martineau, C. *CrystEngComm* **2013**, *15*, 8613−8622.
(118) Martineau, C.; Bouchevreau, B.; Tian, Z.; Lohmeier, S. J.; Behrens, P.; Taulelle, F. *Chem. Mater.* **2011**, *23*, 4799−4809.
(119) Martineau, C.; Mellot-Draznieks, C.; Taulelle, F. *Phys. Chem. Chem. Phys.* **2011**, *13*, 18078−18087.
(120) Beitone, L.; Huguenard, C.; Gansmüller, A.; Henry, M.; Taulelle, F.; Loiseau, T.; Férey, G. *J. Am. Chem. Soc.* **2003**, *125*, 9102−9110.
(121) Morais, C. M.; Montouillout, V.; Deschamps, M.; Iuga, D.; Fayon, F.; Paz, F. A. A.; Rocha, J.; Fernandez, C.; Massiot, D. *Magn. Reson. Chem.* **2009**, *47*, 942−947.
(122) Bull, L. M.; Bussemer, B.; Anupold, T.; Reinhold, A.; Samoson, A.; Sauer, J.; Cheetham, A. K.; Dupree, R. *J. Am. Chem. Soc.* **2000**, *122*, 4948−4958.
(123) Griffin, J. M.; Clark, L.; Seymour, V. R.; Aldous, D. W.; Dawson, D. M.; Iuga, D.; Morris, R. E.; Ashbrook, S. E. *Chem. Sci.* **2012**, *3*, 2293−2300.
(124) He, P.; Xu, J.; Terskikh, V. V.; Sutrisno, A.; Nie, H. Y.; Huang, Y. *J. Phys. Chem. C* **2013**, *117*, 16953−16960.
(125) Loiseau, T.; Serre, C.; Huguenard, C.; Fink, G.; Taulelle, F.; Henry, M.; Bataille, T.; Férey, G. *Chem.—Eur. J.* **2004**, *10*, 1373−1382.
(126) Mowat, J. P. S.; Seymour, V. R.; Griffin, J. M.; Thompson, S. P.; Slawin, A. M. Z.; Fairen-Jimenez, D.; Düren, T.; Ashbrook, S. E.; Wright, P. A. *Dalton Trans.* **2012**, *41*, 3937−3941.
(127) Mowat, J. P. S.; Miller, S. R.; Griffin, J. M.; Seymour, V. R.; Ashbrook, S. E.; Thompson, S. P.; Fairen-Jimenez, D.; Banu, A.-M.; Düren, T.; Wright, P. A. *Inorg. Chem.* **2011**, *50*, 10844−10858.
(128) Kolokolov, D. I.; Jobic, H.; Stepanov, A. G.; Guillerm, V.; Devic, T.; Serre, C.; Férey, G. *Angew. Chem., Int. Ed.* **2010**, *49*, 4791−4794.
(129) Loewenstein, W. *Am. Mineral.* **1953**, *39*, 92−96.
(130) Stebbins, J. F.; Farnan, I.; Williams, E. H.; Roux, J. *Phys. Chem. Mineral.* **1989**, *16*, 763−766.
(131) Stebbins, J. F. *Am. Mineral.* **1997**, *81*, 1315−1320.
(132) Frost, D. J.; Poe, B. T.; Tronnes, R. G.; Liebske, C.; Duba, A.; Rubie, D. C. *Phys. Earth Planet. Inter.* **2004**, *143*−*144*, 507−514.
(133) Griffin, J. M.; Berry, A. J.; Frost, D. J.; Wimperis, S.; Ashbrook, S. E. *Chem. Sci.* **2013**, *4*, 1523−1538.
(134) Eckert, H. *eMagRes* **2007**, DOI: 10.1002/9780470034590.emrstm0009.
(135) Florian, P.; Vermillion, K. E.; Grandinetti, P. J.; Farnan, I.; Stebbins, J. F. *J. Am. Chem. Soc.* **1996**, *118*, 3493−3497.
(136) Farnan, I.; Grandinetti, P. J.; Baltisberger, J. H.; Stebbins, J. F.; Werner, U.; Eastman, M. A.; Pines, A. *Nature* **1992**, *358*, 31−35.
(137) Dubinsky, E. V.; Stebbins, J. F. *Am. Mineral.* **2006**, *91*, 753−761.
(138) Wu, G. *Biochem. Cell Biol.* **1998**, *76*, 429−442.
(139) Polenova, T.; Lipton, A. S.; Ellis, P. D. *eMagRes* **2011**, DOI: 10.1002/9780470034590.emrstm1222.
(140) Lipton, A. S.; Heck, R. W.; Hernick, M.; Fierke, C. A.; Ellis, P. D. *J. Am. Chem. Soc.* **2008**, *130*, 12671−12679.
(141) Laurencin, D.; Smith, M. E. *Prog. Nucl. Magn. Reson. Spectrosc.* **2013**, *68*, 1−40.
(142) Laurencin, D.; Wong, A.; Chrzanowski, W.; Knowles, J. C.; Qiu, D.; Pickup, D. M.; Newport, R. J.; Gan, Z.; Duer, M. J.; Smith, M. E. *Phys. Chem. Chem. Phys.* **2010**, *12*, 1081−1091.
(143) Pound, R. V. *Phys. Rev.* **1950**, *79*, 685−702.
(144) Frydman, L.; Scherf, T.; Lupulescu, A. *Proc. Natl. Acad. Sci. U.S.A.* **2002**, *99*, 15858−15862.
(145) Takeda, K. *Solid State Nucl. Magn. Reson.* **2012**, *47*−*48*, 1−9.
(146) Wind, R. A. *eMagRes* **2007**, DOI: 10.1002/9780470034590.emrstm0140.

(147) Blanc, F.; Sperrin, L.; Jefferson, D. A.; Pawsey, S.; Rosay, M.; Grey, C. P. *J. Am. Chem. Soc.* **2013**, *135*, 2975−2978.
(148) Lee, D.; Takahashi, H.; Thankamony, A. S. L.; Dacquin, J. P.; Bardet, M.; Lafon, O.; Paëpe, G. *J. Am. Chem. Soc.* **2012**, *134*, 18491−18494.
(149) Vitzthum, V.; Miéville, P.; Carnevale, D.; Caporini, M. A.; Gajan, D.; Copéret, C.; Lelli, M.; Zagdoun, A.; Rossini, A. J.; Lesage, A.; Emsley, L.; Bodenhausen, G. *Chem. Commun.* **2012**, *48*, 1988−1990.
(150) Pickard, C. J.; Needs, R. J. *J. Phys.: Condens. Mater.* **2011**, *23*, No. 053201.
(151) Zheng, A.; Huang, S. J.; Wang, Q.; Zhang, H.; Deng, F.; Liu, S. B. *Chin. J. Catal.* **2013**, *34*, 436−491.
(152) Roberts, S. T.; Renshaw, M. P.; Lutecki, M.; McGregor, J.; Sederman, A. J.; Mantle, M. D.; Gladden, L. F. *Chem. Commun.* **2013**, *49*, 10519−10521.